

1 **Galectin-7 impairs placentation and causes preeclampsia features in mice**

2 Ellen Menkhorst^{1,2,3,*}, Wei Zhou^{1,2}, Leilani Santos^{1,2}, Sarah Delforce^{4,5,6}, Teresa So^{1,2}, Kate
3 Rainczuk³, Hannah Loke³, Argyro Syngelaki⁷, Swati Varshney⁸, Nicholas Williamson⁸, Kirsty
4 Pringle^{4,5,6}, Morag J. Young^{9,10,^}, Kypros Nicolaides⁷, Yves St-Pierre¹¹, Eva Dimitriadis^{1,2,3,12,*}

5 ¹Department of Obstetrics and Gynaecology, The University of Melbourne, Parkville, VIC,
6 Australia

7 ²Gynaecology Research Centre, Royal Women's Hospital, Parkville, VIC, Australia

8 ³Centre for Reproductive Health, Hudson Institute of Medical Research, Clayton, VIC, Australia

9 ⁴School of Biomedical Sciences and Pharmacy, University of Newcastle, Newcastle, NSW,
10 Australia

11 ⁵Priority Research Centre for Reproductive Sciences, University of Newcastle, Newcastle, NSW,
12 Australia

13 ⁶Pregnancy and Reproduction Program, Hunter Medical Research Institute, Newcastle, NSW,
14 Australia

15 ⁷Harris Birthright Research Centre for Fetal Medicine, King's College Hospital, London, United
16 Kingdom

17 ⁸Melbourne Mass Spectrometry and Proteomics Facility, Bio21 Molecular Science &
18 Biotechnology Institute, The University of Melbourne, Melbourne, VIC, Australia

19 ⁹Centre for Endocrinology and Metabolism, Hudson Institute of Medical Research, Clayton, VIC,
20 Australia

21 ¹⁰Baker Heart & Diabetes Institute, Prahran, VIC, Australia

22 ¹¹INRS-Institut Armand-Frappier, Laval, QC, Canada

23 ¹²Department of Anatomy and Developmental Biology, Monash University, Clayton, VIC,
24 Australia

25 *Current address: ^{1,2}

26 ^ Current address: ¹⁰

27

28 Short title: 50 characters

29 High placental galectin-7 precedes preeclampsia

30

31 Corresponding author: Eva Dimitriadis, Level 7, Royal Women's Hospital, 20 Flemington Rd,
32 Parkville, VIC, Australia, 3052; Phone: +61 3 8345 2215; email: eva.dimitriadis@unimelb.edu.au

33 The authors have declared that no conflict of interest exists.

34

35 **Abstract**

36 Preeclampsia is a serious pregnancy-induced disorder unique to humans. The etiology of
37 preeclampsia is poorly understood, however poor placental formation is thought causal.
38 Galectin-7 is produced by trophoblast and is elevated in first-trimester serum of women who
39 subsequently develop preeclampsia. We hypothesized that elevated placental galectin-7 may be
40 causative of preeclampsia. Here we demonstrated increased galectin-7 production in chorionic
41 villous samples from women who subsequently develop preterm preeclampsia compared to
42 uncomplicated pregnancies. *In vitro*, galectin-7 impaired human first-trimester trophoblast
43 outgrowth, increased placental production of the anti-angiogenic sFlt-1 splice variant, *sFlt-1-e15a*
44 and reduced placental production and secretion of ADAM12 and angiotensinogen. *In vivo*,
45 galectin-7 administration (E8-E12) to pregnant mice caused elevated systolic blood pressure,
46 albuminuria, impaired placentation (reduced labyrinth vascular branching, impaired decidual
47 spiral artery remodeling and a pro-inflammatory placental state demonstrated by elevated IL1 β ,
48 IL6 and reduced IL10) and dysregulated expression of renin-angiotensin system components in
49 the placenta, decidua and kidney, including angiotensinogen, prorenin and the angiotensin II type
50 1 receptor. Collectively, this study demonstrates that elevated galectin-7 during placental
51 formation contributes to abnormal placentation and suggests it leads to the development of
52 preeclampsia via altering placental production of sFlt-1 and renin-angiotensin system
53 components. Targeting galectin-7 may be a new treatment option for preeclampsia.

54

55

56 **Key words.**

57 Galectin-7, chorionic villous samples, preeclampsia, renin-angiotensin system, sFlt-1-e15a,

58 ADAM12, placentation.

59

60 **Introduction**

61 Preeclampsia is a serious pregnancy-induced disorder unique to humans. With a worldwide
62 incidence of 4.6% of pregnancies¹, over 4 million women develop preeclampsia each year,
63 claiming the lives of 100,000 women and 500,000 babies² and increasing long-term chronic
64 disease risk in both mother and child¹.

65 Preeclampsia manifests clinically as a complex multi-system disease¹ diagnosed by sudden onset
66 hypertension (>20 weeks gestation) and at least one associated complication (proteinuria, other
67 maternal organ dysfunction or fetal growth restriction)³. Poor placentation during the first-
68 trimester is thought the underlying cause of preeclampsia, however its etiology in relation to
69 time of disease onset is unclear^{1, 4}. During placentation, extravillous trophoblast (EVT) invade
70 from anchoring placental villi into the decidua, remodeling uterine spiral arterioles to create high
71 flow, low resistance vessels. This process is maximal in the first-trimester but continues until ~18
72 weeks gestation⁵. The placental villi are bathed in maternal blood into which they release a
73 wealth of factors which reflect placental function¹. If the placenta is abnormal it can release toxic
74 factors which damage maternal vasculature¹. The abnormal placenta also has dysregulated
75 expression of renin-angiotensin system (RAS) components which in turn may lead to activation
76 of the maternal intrarenal RAS and failure of the circulating renin-angiotensin-aldosterone-
77 system (RAAS) to respond appropriately to the homeostatic demands of pregnancy⁶.

78 Galectins are animal (soluble) lectins abundantly expressed at the maternal-fetal interface⁷.

79 Galectins bind to surface glycoproteins (preferentially β -galactoside) and have many functions

80 critical for placentation including cell invasion and immune tolerance⁷: dysregulated expression
81 of galectins-1,3,9 and 13 is associated with preeclampsia⁷⁻¹¹.

82 Galectin-7 is expressed by first-trimester syncytiotrophoblast and EVT^{12, 13}, but the function of
83 galectin-7 during placentation is unknown. Galectin-7 has many functions including roles in cell
84 adhesion¹⁴, migration¹⁵⁻¹⁷ and immune cell regulation¹⁸, all key functions during placentation.
85 *Lgals7* deficient mice are fertile and give rise to normal and fertile offspring¹⁹. Galectin-7 acts
86 intracellularly, via interactions with Ras²⁰ or Bcl-2²¹, and extracellularly via paracrine mechanisms
87 to induce gene transcription^{22, 23}. Galectin-7 is abnormally elevated in first-trimester serum from
88 women who subsequently develop preeclampsia¹². We hypothesized that elevated placental
89 galectin-7 may play a causative role in the development of preeclampsia.

90

91

92 **METHODS**

93 The authors declare that all supporting data are available within the article, its online
94 supplementary files and the mass spectrometry proteomics data have been deposited to the
95 ProteomeXchange Consortium via the PRIDE²⁴ partner repository with the dataset identifier
96 PXD019331.

97 **Primary tissue isolation and culture**

98 Human placental tissue was collected under appropriate Human Research and Ethics Committee
99 approvals (Monash Health and the Royal Women's Hospital, Melbourne #09317B; King's College
100 Hospital, London REC:03-04-070). Written and informed consent was obtained from each patient
101 before surgery.

102 First and second-trimester placental villous and decidua tissue was donated by healthy women
103 undergoing pregnancy termination for psychosocial reasons (amenorrhea 6-22 weeks; n=82).
104 First trimester placenta were cultured as described in the supplementary methods. Briefly, EVT
105 were isolated from cytotrophoblast²⁵ for gelatin zymography²⁶, villous explants were cultured for
106 RT-qPCR or mass spectrometry^{27, 28} or extravillous trophoblast outgrowth²⁹.

107 Chorionic villous samples (CVS, n=20) taken from women undergoing screening for fetal
108 chromosomal abnormalities were snap frozen immediately after collection. Patient
109 characteristics are shown in Supplementary Methods and Tables S1&S2.

110 **In vivo mouse experiments**

111 All procedures were approved by the Monash Medical Centre (B) (#MMCB2016/07) and
112 Melbourne University (#1814697) Animal Ethics Committees. This study followed the NHMRC
113 Australian Code of Practice for the Care and Use of Animals for Scientific Purposes.

114 Recombinant galectin-7 administration

115 Mated female C57BL6 mice received sub-cutaneous injections of 400µg/kg/day galectin-7 or
116 vehicle control from E8 (E, embryonic day; plug detection, E0) to E12, or 5 consecutive days in
117 non-pregnant mice. Systolic Blood Pressure (sBP) was measured by tail-cuff plethysmography²⁹.
118 Pregnant mice were killed on E13, E17 or allowed to pup (n=5-6/group). Tissues, urine and serum
119 collected were subjected to gene array, RT-qPCR, ELISA, placental morphometry³⁰, histology and
120 immunohistochemistry as detailed in supplementary data.

121

122 Statistics

123 Statistical analyses were performed by GraphPad Prism version 8.3.1. $P < 0.05$ was considered
124 significant. Data were tested for normality and statistical tests (indicated in figure legends)
125 chosen according to experimental design.

126

127 **RESULTS**

128 **Galectin-7 is elevated in human placenta from pregnancies that subsequently develop preterm**
129 **preeclampsia.**

130 Galectin-7 is produced by first- and second-trimester placental villi^{12, 13} and decidua (Figure
131 S1A&B). Galectin-7 production did not change across gestation, except for a significant increase
132 in placental villi *LGALS7* expression at 10 weeks gestation (Figure S1A&B). Elevated placental
133 galectin-7 was found in CVS from women who subsequently developed preterm preeclampsia
134 compared to uncomplicated controls (Figure 1A&B). Galectin-7 immunolocalized predominantly
135 to syncytiotrophoblast cytoplasm (Figure 1B).

136 Galectin-7 treatment inhibited EVT outgrowth from first-trimester placental villi (Figure 1C) and
137 increased production of *SFLT-1-E15A* (Figure 1D), a primate, placental-specific splice variant of
138 sFlt-1 augmented during preeclampsia³¹. There was no effect of galectin-7 on the conserved full-
139 length *FLT-1* (Figure 1E).

140 **Galectin-7 induced the features of preeclampsia in mice.**

141 The human data presented above strongly implicates galectin-7 in the etiology of preeclampsia.
142 Therefore, we investigated whether elevating galectin-7 during placental formation in mice
143 induced features of preeclampsia.

144 Because galectin-7 has not previously been localized to mouse implantation sites we first
145 examined galectin-7 production in implantation sites across gestation. Galectin-7 protein
146 increased across gestation peaking in the decidua and metrial lymphoid aggregate of pregnancy
147 (MLAp) compartment at E15 and E17 compared to E6 implantation site (Figure S2A) and was

148 significantly higher in E15&17 decidua and MLAp compared to E15&17 placenta (Figure S2A).
149 Galectin-7 immunolocalization was predominantly intracellular and strongly localized to E6
150 myometrium and E13/16 MLAp and fetus and weakly immunolocalized to E13/16 labryinth
151 (Figure S2B).

152 To model the profile of elevated serum galectin-7 only during early pregnancy (the period of
153 maximal placentation) of women who subsequently develop preeclampsia¹², we injected
154 galectin-7 to pregnant mice from E8-12, to elevate galectin-7 during the period of maximal
155 placentation in mice (E9-E14)³². This significantly increased serum galectin-7 concentration at E13
156 but not E17 (Figure S3A). There was no change in placental or decidual galectin-7 levels (Figure
157 S3B).

158 This transient augmentation of circulating galectin-7 elevated systolic blood pressure (sBP)
159 (Figure 2A) and increased urinary albumin/creatinine ratio (Figure 2B) in pregnant mice but had
160 no effect in non-pregnant mice. Galectin-7 treatment had no effect on serum or placental Flt-1
161 (Figure 2C; Figure S3C respectively) or serum sEndoglin (Figure S3D).

162 Galectin-7 treatment had no effect on gestation length (Figure S3E), fetal number (Figure S3F) or
163 fetal bodyweight (Figure 2D). The placental and decidual unit weight was significantly reduced at
164 E13 (not E17; Figure 2E), but the fetal:placenta&decidua unit ratio was unchanged (Figure 2F).
165 Although no fetal growth restriction was observed, reduced pup bodyweight (P7 to P21) was
166 found in pups born from galectin-7 treated dams (Figure 2D).

167 **Galectin-7 altered renin-angiotensin system components.**

168 Using a mouse preeclampsia gene expression array (QIAGEN), we found galectin-7 treatment
169 altered decidual and kidney *Agtr1a* (angiotensin II type 1 receptor) (Tables S3-5). We therefore
170 determined whether galectin-7 treatment altered production of major RAS components *Ace*,
171 *Ace2*, *Agt* (*angiotensinogen*), *Agtr1a*, *Atp6ap2* (prorenin receptor), *Mme* (neprilysin) and *Renin*
172 (Prorenin) (Figure S4). Galectin-7 treated mice showed significantly reduced placental *Agt*
173 expression at E13 (Figure 3A), increased *Agtr1a* expression in the kidney at E13 and placenta and
174 heart at E17 (Figure 3B), altered *Renin* expression at E13 in the decidua (reduced) and kidney
175 (increased; Figure 3C) and increased kidney *Atp6ap2* expression at E13 (Figure 3D). Using human
176 first-trimester placental villi we confirmed that galectin-7 down-regulated Angiotensinogen
177 expression (RT-qPCR; Figure 3E) and secretion (mass spectrometry; Figure 3F; Table S8).

178 **Galectin-7 impaired placental formation in mice.**

179 Galectin-7 administration impaired placental development compared to vehicle control (Figure
180 4A-B): at E13 the labyrinth and junctional zones were smaller and at E17 the decidua was larger
181 (Figure 4A). Labyrinth vascular branching was significantly reduced at E13 in placentas from
182 galectin-7 treated mice. Vascular branching counts fell significantly at E17 compared to E13 and
183 there was no difference between treated and control mice at E17 (Figure 4C).

184 Trophoblast invasion of decidual spiral arteries was not identified in galectin-7 treated E13
185 implantation sites, with no CK7 positive trophoblast visible in α -SMA stained decidual spiral
186 arteries (Figure 4D). Correspondingly, vascular smooth muscle cells were retained around
187 decidual arteries in galectin-7 treated mice (Figure 4E), suggesting galectin-7 significantly
188 impaired decidual spiral artery remodeling. There was no effect of galectin-7 on uterine Natural

189 Killer (uNK) cell number in the decidua (Figure 4F), suggesting although uNK cells are the main
190 mediators of spiral artery remodeling in mice, reduced spiral artery remodeling seen here was
191 due to impaired trophoblast invasion. We did not however investigate uNK phenotype or
192 function.

193 Placentas from galectin-7 treated mice had elevated *Il1b* (Figure 5A) at E13 and elevated *Il6*
194 (Figure 5B) and reduced *Il10* (Figure 5C) at E17.

195 **Galectin-7 altered production of key regulators of trophoblast invasion.**

196 Galectin-7 enhances invasion via MMP9 in other cells^{23, 33}. Here, despite increased MMP9
197 production by human placental villi (Figure 6A&B), galectin-7 inhibited EVT outgrowth (Figure
198 1C), suggesting that galectin-7 inhibits trophoblast invasion via a different mechanism. This
199 hypothesis is supported by our *in vivo* data, where murine placental production of *MMP9* was
200 not significantly altered (Figure S5A), although galectin-7 is active in mouse cells, demonstrated
201 by induction of *Mmp9 in vitro* () (Figure S5B). We have previously shown a similar difference in
202 regulation of invasion between trophoblast and cancer cells with IL11³⁴.

203 To identify the mechanism by which galectin-7 impaired trophoblast invasion we screened
204 factors known to regulate EVT invasion. Galectin-7 significantly inhibited human first-trimester
205 placental villous *a disintegrin and metalloproteinase (ADAM)12* expression (Figure 6C), increased
206 *Pappalysin (PAPPA)2* expression (Figure S5C) but had no effect on *Interleukin (IL)11* expression
207 (Figure S5D). Galectin-7 treatment inhibited human first-trimester inhibited placental villous
208 secretion of ADAM12S (Figure 6D) and correspondingly, reduced murine placental and decidual
209 *Adam12* expression (Figure 6E) and placental ADAM12S production (Figure 6F).

210 **DISCUSSION**

211 We provide evidence that placental galectin-7 was elevated in women who subsequently develop
212 preterm preeclampsia. Augmented galectin-7 during the period of placental formation in mice
213 caused hypertension and albuminuria, likely by disrupting placentation and altering placental
214 expression of angiogenic factors, regulators of trophoblast invasion and cytokines, all known to
215 be involved in the etiology of preeclampsia.

216 CVS offer an unprecedented opportunity to investigate placental alterations and function prior to
217 the onset of preeclampsia. Our CVS data indicates that galectin-7 production is increased in
218 placentas of women who go on to develop preterm preeclampsia and that galectin-7 alters
219 placental expression of genes found in multiple pathways which are associated with
220 preeclampsia. Increased syncytial production of galectin-7 provides strong evidence supporting
221 increased placental release of galectin-7 into maternal blood as we previously found¹². The
222 impact of even slightly increased galectin-7 production may be substantial and sustained: galectin
223 proteins are highly stable due to protease resistance and increased stability following ligand
224 binding³⁵. Moreover, elevated galectin-7 expression is enhanced by an autocrine amplification
225 loop in various epithelial cell types³⁶.

226 Whether decidual production of galectin-7 is likewise altered in preeclampsia is unknown: our
227 CVS samples contained no decidua. A previous microarray study utilizing CVS containing decidua
228 did not investigate *Igals7*³⁷. It is of note that we found no change in galectin-7 production in
229 placental or decidual tissue from weeks 6-22, except in week 10 placental villous and interestingly,
230 this was found only in a subgroup of placentas. This tissue is obtained from terminations, so the

231 pregnancy outcome is unknown. It is possible that placentas with elevated galectin-7 at week 10
232 may have developed preeclampsia, however clinical characteristics which may indicate high-risk
233 of preeclampsia were not recorded.

234 Galectin-7 administration induced hypertension and albuminuria in pregnant mice yet did not
235 alter serum sFlt-1 concentration. It is unsurprising that galectin-7 did not regulate sFlt-1 in mice,
236 as in human placental villi galectin-7 regulated only *sFlt-1-e15a*, the sFlt-1 splice variant present
237 only in the placenta of higher-order primates³¹. sFlt-1-e15a is predominantly produced by the
238 placenta (as opposed to eg. sFlt-1-i13 which is predominantly endothelial) and is proposed as the
239 primary sFlt-1 variant associated with preeclampsia³¹. Mirroring our finding that galectin-7 was
240 elevated only in CVS from preterm preeclampsia pregnancies, sFlt-1-e15a is significantly elevated
241 in maternal plasma from women with early onset preeclampsia³⁸.

242 Our observation that sFlt-1 is not required to induce preeclampsia features in mice has
243 precedence: models generated by TNF α infusion³⁹ and loss of PlGF⁴⁰ show no effect on circulating
244 sFlt-1; moreover nicotinamide rescues preeclampsia features without altering sFlt-1 levels in two
245 mouse models of preeclampsia⁴¹. Taken together, this suggests that at least in mouse models of
246 preeclampsia, hypertension is modulated independent of sFlt-1. Whether sFlt-1/PlGF levels are
247 causal factors in the development of preeclampsia or reflect placental cellular stress is of
248 debate^{40, 42}.

249 In a healthy pregnancy, the maternal renal RAS and circulating RAAS are activated to expand the
250 cardiovascular system, maintain blood pressure and increase renal blood flow. In established
251 preeclampsia alterations to the circulating RAAS and tissue (placental, decidual, renal) RAS are

252 clear^{6, 43}: prorenin, angiotensinogen, angiotensin converting enzyme (ACE) and the angiotensin II
253 type 1 receptor (AT₁R) are all upregulated in the placenta⁴⁴⁻⁴⁶, however the specific alterations to
254 the RAS during placental formation and the effect of these alterations in the pathogenesis of
255 preeclampsia are unknown, in part due to the lack of appropriate models. Galectin-7 treatment
256 altered the expression of multiple RAS genes, including placental *Agt* prior to preeclampsia onset,
257 and placental *Agtr1a* in established preeclampsia. We hypothesise that the initial reduction in
258 *Agt* may reduce angiotensin II production, thus inhibiting trophoblast invasion and spiral artery
259 remodelling early in pregnancy. Conversely, increased placental AT₁R in established preeclampsia
260 may be in response to oxidative stress and further compromise uteroplacental blood flow. Further
261 experiments, particularly activity assays (eg ACE) are required to prove that the RAAS and tissue
262 RAS are dysregulated in galectin-7 treated mice. We also found that galectin-7 reduced *Agt*
263 expression and angiotensinogen secretion in human first-trimester placental villi, supporting a
264 role for galectin-7 in regulating RAS components in human placenta.

265 Preeclampsia is associated with increased sensitivity to Ang II⁴⁷. Alterations in circulating
266 angiotensin peptides may alter vascular sensitivity to Ang II or activate other maternal RASs such
267 as the intrarenal RAS: indeed, kidney RAS gene expression was altered in galectin-7 treated mice.
268 To the best of our knowledge this is the only *in vivo* model of preeclampsia which displays
269 alterations to the RAS without imposing direct changes on RAS components or the uterine
270 vasculature. This model could be useful to understand the role of the RAS in the aetiology of
271 preeclampsia.

272 Whilst we found no effect of galectin-7 on the development of hypertension or albuminuria in
273 non-pregnant mice, RAS gene expression was altered in the peripheral organs of pregnant mice.

274 Future studies could be determine whether galectin-7 is upregulated in hypertension or
275 cardiovascular disease.

276 Intriguingly, in women with established preeclampsia the placenta at the time of delivery is very
277 often not morphologically abnormal⁴⁸: here we found that although the E13 placenta was
278 morphologically abnormal, the E17 placenta was morphologically normal with restored weight
279 and labyrinth vascular branching. Despite this, our gene expression data demonstrated that
280 placental function likely remained altered, as evidenced by elevated *Il6* and *Agtr1a* and reduced
281 *Il10* expression. Elevated placental IL1 β , IL6 and reduced IL10 is found in women with
282 preeclampsia⁴⁹⁻⁵² and likely reflects a pro-inflammatory placental state. Galectin-7 is reported to
283 induce T cell polarization towards Th1, including reduced IL10 production¹⁸ however to our
284 knowledge this is the first report of galectin-7 stimulating *Il1 β* and *Il6* expression.

285 Galectin-7 is a well-established regulator of cell movement, promoting migration/invasion in
286 many epithelial and epithelial cancer cells^{15-17, 23, 33}. Here we found galectin-7 treatment impaired
287 trophoblast invasion/outgrowth *in vivo* and *in vitro*. Galectin-7 inhibition of invasion has only
288 previously been reported in prostate cancer⁵³. In this study we have identified for the first time
289 that galectin-7 impairs human trophoblast invasion likely via ADAM12 and PAPP2. ADAM
290 proteins are multidomain molecules which have multiple critical functions including promoting
291 cell proliferation, survival, migration and invasion. ADAM12 has 2 alternatively spliced variants,
292 ADAM12L, a transmembrane isoform and ADAM12S, a secreted isoform. ADAM12 localizes to
293 human villous and extravillous trophoblast and promotes outgrowth *in vitro*^{54, 55}. In this study we
294 demonstrated that ADAM12S protein production was significantly down-regulated in placentas
295 of galectin-7 treated mice. ADAM12S promotes human trophoblast invasion *in vitro*^{54, 55}.

296 Whether ADAM12 regulates trophoblast invasion in mice is unknown, however reduced
297 trophoblast invasion in galectin-7 treated placentas was associated with lower placental *ADAM12*
298 production. ADAM12S promotes murine endometrial stromal cell decidualization⁵⁶ however we
299 saw no effect of galectin-7 treatment on the decidualization or decidual production of ADAM12S,
300 likely as galectin-7 treatment did not begin until E8, when decidualization is essentially
301 complete⁵⁷.

302 Reduced circulating ADAM12S is found in women who subsequently develop preeclampsia^{58, 59}.
303 Circulating ADAM12S at 20 weeks gestation is a better predictor of subsequent preeclampsia in
304 pregnancies with a male fetus than a female⁶⁰. The preterm CVS samples were all from
305 pregnancies with male fetuses and 5/6 term CVS samples were from pregnancies with female
306 fetuses. Whether placental gender has an effect on galectin-7 production in preeclampsia is
307 unknown but should be considered as other galectins show gender-dependent expression
308 patterns in intra-uterine growth restriction⁶¹ and we previously found that galectin-7 is also
309 upregulated in prospective sera from women who developed term preeclampsia¹².

310

311 **PERSPECTIVES**

312 Overall, this study demonstrates that galectin-7 may play a significant role in the initiation of
313 preeclampsia: via impaired placental formation, placental inflammation and placental release of
314 anti-angiogenic factors. As galectin-7 induced hypertension and albuminuria only in pregnant
315 mice, we hypothesize that in women, galectin-7 acts via the placenta to induce the systemic
316 features of preeclampsia. There are few mouse models of preeclampsia driven by the placenta²⁹,
317 and none that display RAS dysregulation without direct alterations to RAS components or uterine

318 vasculature, thus this *in vivo* model of preeclampsia will be of significant utility to understand the
319 mechanisms leading to preeclampsia and to test therapeutics in pre-clinical trials. Galectin-7 may
320 be a therapeutic target to normalise placental function during mid-gestation, and in combination
321 with other risk factors, a novel biomarker to identify women at risk of developing preeclampsia.
322

323 **Acknowledgements.**

324 We are grateful to the women who donated tissue; Sr. Judi Hocking, Sr. Emily-Jane Bromley, Dr
325 Ian Roberts, Dr Paddy Moore and Dr Jeanette Henderson and Animal Facility staff. We thank Kelli
326 Sorby, Dr Masashi Takamura, and Dr Amy Winship for technical assistance.
327

328 **Sources of funding.**

329 Funding: NHMRC (Australia) Project/Program Grant (GNT1098332) and Fellowships (#550905;
330 ED) (#611827; EM); Rebecca L Cooper Medical Research Foundation Project Grant; Trevor B
331 Kilvington Bequest Foundation and the Victorian Government's Operational Infrastructure
332 Support Program.
333

334 **Disclosure.**

335 The authors have nothing to declare.

336 **References**

- 337 1. Burton GJ, Redman CW, Roberts JM, Moffett A. Pre-eclampsia: Pathophysiology and
338 clinical implications. *BMJ*. 2019;366:l2381
- 339 2. Ostyon C, Stanley J, Barker P. Potential targets for the treatment of preeclampsia. *Expert*
340 *Opin Ther Targets*. 2015;19:15117-11530
- 341 3. Tranquilli AL, Dekker G, Magee L, Roberts J, Sibai BM, Steyn W, Zeeman GG, Brown MA.
342 The classification, diagnosis and management of the hypertensive disorders of
343 pregnancy: A revised statement from the ISSHP. *Pregnancy Hypertension*. 2014;4:97-104
- 344 4. Stepan H, Hund M, Andraczek T. Combining biomarkers to predict pregnancy
345 complications and redefine preeclampsia. *Hypertension*. 2020;75:918-926
- 346 5. Redman CW, Sargent IL. Latest advances in understanding preeclampsia. *Science*.
347 2005;308:1592-1594
- 348 6. Lumbers ER, Delforce SJ, Arthurs AL, Pringle KG. Causes and consequences of the
349 dysregulated maternal renin-angiotensin system in preeclampsia. *Frontiers in*
350 *Endocrinology*. 2019;10
- 351 7. Than NG, Romero R, Balogh A, Karpati E, Mastrolia SA, Staretz-Chacham O, Hahn S, Erez
352 O, Papp Z, Kim CJ. Galectins: Double-edged swords in the cross-roads of pregnancy
353 complications and female reproductive tract inflammation and neoplasia. *Journal of*
354 *Pathology and Translational Medicine*. 2015;49:181-208
- 355 8. Hao H, He M, Li J, Zhoy Y, Dang J, Li F, Yang M, Deng D. Upregulation of the tim-3/gal-9
356 pathway and correlation with the development of preeclampsia. *European Journal of*
357 *Obstetrics, Gynecology and Reproductive Biology*. 2015;194:85-91

- 358 9. Freitag N, Tirado-Gonzalez I, Barrientos G, Herse F, Thijssen VLJL, Weedon-Fekjaer SM,
359 Schulz H, Wallukat G, Klapp BF, Nevers T, Sharma S, Staff AC, Dechend R, Blois SM.
360 Interfering with gal-1-mediated angiogenesis contributes to the pathogenesis of
361 preeclampsia. *Proceedings of the National Academy of Sciences*. 2013;110:11451-11456
- 362 10. Li ZH, Wang LL, Liu H, Muyayalo KP, Huang XB, Mor G, Lao AH. Galectin-9 alleviates lps-
363 induced preeclampsia-like impairment in rats via switching decidual macrophage
364 polarization to m2 subtype. *Frontiers in Immunology*. 2019;9:3142
- 365 11. Than NG, Erez O, Wildman DE, Tarca AL, Edwin SS, Abbas A, Hotra J, Kusanovic JP,
366 Gotsch F, Hassan SS, Espinoza J, Papp Z, Romero R. Severe preeclampsia is characterized
367 by increased placental expression of galectin-1. *Journal of maternal-fetal and neonatal
368 medicine*. 2008;21:429-442
- 369 12. Menkhorst EM, Koga K, Van Sinderen M, Dimitriadis E. Galectin-7 serum levels are
370 altered prior to the onset of pre-eclampsia. *Placenta*. 2014;35:281-285
- 371 13. Unverdorben L, Jesche U, Santoso L, Hofmann S, Kuhn C, Arck P, Hutter S. Comparative
372 analyses on expression of galectins1-4, 7-10 and 12 in first trimester placenta, decidua
373 and isolated trophoblast cells *in vitro*. *Histol Histopathol*. 2016;31:1095-1111
- 374 14. Menkhorst EM, Gamage T, Cuman C, Kaitu'u-Lino TJ, Tong S, Dimitriadis E. Galectin-7
375 acts as an adhesion molecule during implantation and increased expression is associated
376 with miscarriage. *Placenta*. 2014;35:195-201
- 377 15. Cao Z, Said N, Amin S, Wu HK, Bruce A, Garate M, Hsu DK, Kuwabara I, Liu F-T, Panjwani
378 N. Galectins-3 and -7, but not galectin-1, play a role in re-epithelialization of wounds.
379 *Journal of Biological Chemistry*. 2002;277:42299-42305

- 380 16. Menkhorst EM, Griffith M, Van Sinderen M, Niven K, Dimitriadis E. Galectin-7 is elevated
381 in endometrioid (type 1) endometrial cancer and promotes cell migration. *Oncology*
382 *Letters*. 2018;16:4721-4728
- 383 17. Evans J, Yap J, Gamage T, Salamonsen LA, Dimitriadis E, Menkhorst EM. Galectin-7 is
384 important for normal uterine repair following menstruation. *Molecular Human*
385 *Reproduction*. 2014;20:787-798
- 386 18. Luo Z, Ji Y, Tian D, Zhang Y, Chang S, Yang C, Zhou H, Chen ZK. Galectin-7 promotes
387 proliferation and th1/2 cells polarization toward th1 in activated cd4+ t cells by
388 inhibiting the $\text{tgf}\beta/\text{smad3}$ pathway. *Molecular Immunology*. 2018;101:80-85
- 389 19. Gendronneau G, Sidhy SS, Delacour D, Dang T, Calonne C, Houzelstein D, Magnaldo T,
390 Poirier F. Galectin-7 in the control of epidermal homeostasis after injury. *Mol. Biol. Cell*.
391 2008;19:5541-5549
- 392 20. Kuwabara I, Kuwabara Y, Yang R-Y, Schuler M, Green DR, Zuraw BL, Hsu DK, Liu F-T.
393 Galectin-7 exhibits pro-apoptotic function through jnk activation and mitochondrial
394 cytochrome c release. *Journal of Biological Chemistry*. 2002;277:3487-3497
- 395 21. Villeneuve C, Baricault L, Canelle L, Barboule N, Racca C, Monsarrat B, Magnaldo T,
396 Larminat F. Mitochondrial proteomic approach reveals galectin-7 as a novel bcl-2
397 binding protein in human cells. *Mol Biol Cell*. 2011;22
- 398 22. Rabinovich GA, Toscano MA. Turning 'sweet' on immunity: Galectin-glycan interactions
399 in immune tolerance and inflammation. *Nature Reviews Immunology*. 2009;9:338-352

- 400 23. Demers M, Magnaldo T, St-Pierre Y. A novel function for galectin-7: Promoting
401 tumorigenesis by up-regulating mmp-9 gene expression. *Cancer Research*.
402 2005;65:5205-5210
- 403 24. Perez-Riverol Y, Csordas A, Bai J, Bernal-Llinares M, Hewapathirana S, D.J K, Inuganti A,
404 Griss J, Mayer G, Eisenacher M, et al. The pride database and related tools and
405 resources in 2019: Improving support for quantification data. *Nucleic Acids Res*
406 2019;47:D442-D450
- 407 25. Menkhorst EM, Lane N, Winship A, Li P, Yap J, Meehan K, Rainczuk A, Stephens AN,
408 Dimitriadis E. Decidual-secreted factors alter invasive trophoblast membrane and
409 secreted proteins implying a role for decidual cell regulation of placentation. *PLoS ONE*.
410 2012;7:e31418
- 411 26. Paiva P, Salamonsen LA, Manuelpillai U, Dimitriadis E. Interleukin 11 inhibits human
412 trophoblast invasion indicating a likely role in the decidual restraint of trophoblast
413 invasion during placentation. *BOR*. 2009;80:302-210
- 414 27. Dagley LF, Infusini G, Larsen RH, Sandow JJ, Webb AI. Universal solid-phase protein
415 preparation for bottom-up and top-down proteomics. *Journal of Proteome Research*.
416 2019;18:2915-2924
- 417 28. Hughes CS, Moggridge S, Müller T, Sorensen PH, Morin GB, Krijgsveld J. Single-pot, solid-
418 phase-enhanced sample preparation for proteomics experiments. *Nature Protocols*.
419 2019;14:68-85

- 420 29. Winship AL, Koga K, Menkhorst E, Van Sinderen M, Rainczuk K, Nagai M, Cuman C, Yap J,
421 Zhang J-G, Simmons D, Young MJ, Dimitriadis E. Interleukin-11 alters placentation and
422 causes preeclampsia features in mice. *PNAS*. 2015;112:15928-15933
- 423 30. Garcia-Gonzalez MA, Outeda P, Zhou Q, Zhou F, Menezes LF, Qian F, Huso DL, Germino
424 GG, Piontek KB, Watnick T. Pkd1 and pkd2 are required for normal placental
425 development. *PLoS ONE*. 2010;5:e12821
- 426 31. Palmer KR, Tong S, Kaitu'u-Lino TJ. Placental-specific sflt-1: Role in pre-eclamptic
427 pathophysiology and its translational possibilities for clinical prediction and diagnosis.
428 *Molecular Human Reproduction*. 2017;23:69-78
- 429 32. Hemberger M, Hanna CW, Dean W. Mechanisms of early placental development in
430 mouse and humans. *Nature Reviews Genetics*. 2020;21:27-43
- 431 33. Park JE, Chang WY, Cho M. Induction of matrix metalloproteinase-9 by galectin-7
432 through p38 mapk signaling in hela human cervical epithelial adenocarcinoma cells.
433 *Oncology Reports*. 2009;22:1371-1379
- 434 34. Winship A, Menkhorst E, Van Sinderen M, Dimitriadis E. Interleukin 11: Similar or
435 opposite roles in female reproduction and reproductive cancer? *Reproduction, Fertility
436 and Development*. 2016;28:395-405
- 437 35. Cummings RD, Liu F-T. Galectins. In: Varki A, Cummings RD, Esko JD, Freeze HH, Stanley
438 P, Bertozzi CR, Hart GW, Etzler ME, eds. *Essentials of glycobiology*. Cold Spring Harbor
439 (NY): Cold Spring Harbor Laboratory Press; 2009.

- 440 36. Bibens-Laulan N, St-Pierre Y. Intracellular galectin-7 expression in cancer cell results
441 from an autocrine transcriptional mechanism and endocytosis of extracellular galectin-
442 7. *PLoS ONE*. 2017;12:e0187194
- 443 37. Founds SA, Conley YP, Lyons-Weiler JF, Jeyabalan A, Hogge WA, Conrad KP. Altered
444 global gene expression in first trimester placentas of women destined to develop
445 preeclampsia. *Placenta*. 2009;30:15-24
- 446 38. Palmer KR, Kaitu'u-Lino TJ, Cannon P, Tuohey L, De Silva MS, Varas-Godoy M, Acuña S,
447 Galaz J, Tong S, Illanes SE. Maternal plasma concentrations of the placental specific sflt-1
448 variant, sflt-1 e15a, in fetal growth restriction and preeclampsia. *The Journal of*
449 *Maternal-Fetal & Neonatal Medicine*. 2017;30:635-639
- 450 39. Bobek G, Surmon L, Mirabito KM, Makris A, Hennessy A. Placental regulation of
451 inflammation and hypoxia after tnf- α infusion in mice. *American Journal of Reproductive*
452 *Immunology*. 2015;74:407-418
- 453 40. Parchem JG, Kanasaki K, Kanasaki M, Sugimoto H, Xie L, Hamano Y, Lee SB, Gattone VH,
454 Parry S, Strauss JF, et al. Loss of placental growth factor ameliorates maternal
455 hypertension and preeclampsia in mice. *The Journal of Clinical Investigation*.
456 2018;128:5008-5017
- 457 41. Wang Y, Lv Y, Gao S, Zhang Y, Sun J, Gong C, Chen X, Li G. MicroRNA profiles in
458 spontaneous decidualized menstrual endometrium and early pregnancy decidua with
459 successfully implanted embryos. *PLoS ONE*. 2016;11:e0143116

- 460 42. Redman CWG, Staff AC. Preeclampsia, biomarkers, syncytiotrophoblast stress, and
461 placental capacity. *American Journal of Obstetrics and Gynecology*. 2015;213:S9.e1-
462 S9.e4
- 463 43. Herse F, Dechend R, Harsem N, Wallukat G. Dysregulation of the circulating and tissue-
464 based renin-angiotensin system in preeclampsia. *Hypertension*. 2007;49:604-611
- 465 44. Anton L, Brosnihan K. Systemic and uteroplacental renin-angiotensin system in normal
466 and pre-eclamptic pregnancies. *Ther Adv Cardiovasc Dis*. 2008;2:349-362
- 467 45. Ito S, Itakura A, Ohno Y, Nomura M, Senga T, Nagasaka T, Mizutani S. Possible activation
468 of the renin-angiotensin system in the feto-placental unit in preeclampsia. *J Clin*
469 *Endocrinol Metab*. 2002;87:1871-1878
- 470 46. Anton L, Merrill D, Neves L, Diz D, Corthorn J, Valdes G, Stovall K, Gallagher P,
471 Moorefield C, Gruver C, Brosnihan K. The uterine placental bed renin-angiotensin
472 system in normal and preeclamptic pregnancy. *Endocrinology*. 2009;150:4316-4325
- 473 47. Hariharan N, Shoemaker A, Wagner S. Pathophysiology of hypertension in preeclampsia.
474 *Microvascular Research*. 2017;109:34-37
- 475 48. Falco ML, Sivanathan J, Laoreti A, Thilaganathan B, Khalil A. Placental histopathology
476 associated with pre-eclampsia: Systematic review and meta-analysis. *Ultrasound in*
477 *Obstetrics & Gynecology*. 2017;50:295-301
- 478 49. Bernardi FC, Felisberto F, Vuolo F, Petronilho F, Souza DR, Luciano TF, C.T dS, Ritter C,
479 Dal-Pizzol F. Oxidative damage, inflammation, and toll-like receptor 4 pathway are
480 increased in preeclamptic patients: A case-control study. *Oxidative medicine and cellular*
481 *longevity*. 2012;2012:636419

- 482 50. Zhang Z, Gao Y, Zhang L, Jia L, Wang P, Zhang L, Li H. Alterations of il-6, il-6r and gp130 in
483 early and late onset severe preeclampsia. *Hypertension in Pregnancy*. 2013;32:270-280
- 484 51. Daneva AM, Hadzi-Lega M, Stefanovic M. Correlation of the system of cytokines in
485 moderate and severe preeclampsia. *Clinical and Experimental Obstetrics & Gynecology*.
486 2016;43:220-224
- 487 52. Amash A, Holcberg G, Sapir O, Huleilel M. Placental secretion of interleukin-1 and
488 interleukin-1 receptor antagonist in preeclampsia: Effect of magnesium sulfate. *Journal*
489 *of Interferon & Cytokine Research*. 2012;32:432-441
- 490 53. Labrie M, Vladioiu MC, Leclerc BG, Grosset AA, Gaboury L, Stagg J, St-Pierre Y. A
491 mutation in the carbohydrate recognition domain drives a phenotypic switch in the role
492 of galectin-7 in prostate cancer. *PLoS ONE*. 2015;10:e0131307
- 493 54. Aghababaei M, Perdu S, Irvine K, Beristain AG. A disintegrin and metalloproteinase 12
494 localizes to invasive trophoblast, promotes cell invasion and directs column outgrowth
495 in early placental development. *Molecular Human Reproduction*. 2014;20:235-249
- 496 55. Biadasiewicz K, Fock V, Dekan S, Proestling K, Velicky P, Haider S, Knofler M, Frolich C,
497 Pollheimer J. Extravillous trophoblast-associated adam12 exerts pro-invasive properties
498 including induction of integrin beta 1-mediated cellular spreading. *Biology of*
499 *Reproduction*. 2014;90:101
- 500 56. Zhang L, Guo W, Chen Q, Fan X, Zhang Y, Duan E. Adam12 plays a role during uterine
501 decidualization in mice. *Cell and Tissue Research*. 2009;338:413-421
- 502 57. Edwards AK, Janzen-Pang J, Peng A, Tayade C, Carniato A, Yamada A, Lima P, Tse.
503 Microscopic anatomy of the pregnant mouse uterus during gestation. In: Croy BA,

- 504 Yamada AT, DeMayo FJ, Adamson SL, eds. *The guide to the investigation of mouse*
505 *pregnancy*. Academic Press; 2014:43-67.
- 506 58. Yu N, Cui H, Chen X, Chang Y. First trimester maternal serum analytes and second
507 trimester uterine artery doppler in the prediction of preeclampsia and fetal growth
508 restriction. *Taiwan Journal of obstetrics & gynecology*. 2017;56:358-361
- 509 59. Kasimis C, Evangelinakis N, Rotas M, Georgitsi M, Pelekanos N, Kassanos D. Predictive
510 value of biochemical marker adam-12 at first trimester of pregnancy for hypertension
511 and intrauterine growth restriction. *Clinical and Experimental Obstetrics & Gynecology*.
512 2016;43:43-47
- 513 60. Myers JE, Thomas G, Tuytten R, Van Herrewege Y, Djiokop RO, Roberts CT, Kenny LC,
514 Simpson NAB, North RA, Baker PN. Mid-trimester maternal adam12 levels differ
515 according to fetal gender in pregnancies complicated by preeclampsia. *Reproductive*
516 *sciences* 2015;22:235-241
- 517 61. Hutter S, Knabl J, Andergassen U, Hofmann S, Kuhn C, Mahner S, Arck P, Jeschke U.
518 Placental expression patterns of galectin-1, galectin-2, galectin-3 and galectin-13 in
519 cases of intrauterine growth restriction *International journal of molecular sciences*.
520 2016;17:523-523

521

522

523 **Novelty and Significance**

524 What is new?

525 The identification of galectin-7 as a placental driver of preeclampsia.

526 New mouse model of preeclampsia with dysregulated renin-angiotensin system.

527 What is relevant?

528 Preeclampsia is a disorder of pregnancy characterized by de novo hypertension
529 and increased risk of chronic hypertension later in life.

530 Galectin-7 regulated expression of the renin-angiotensin system.

531 Summary

532 Placental galectin-7 production is increased in women who subsequently
533 develop preterm preeclampsia. In vitro and in vivo studies demonstrate that
534 galectin-7 is a likely driver of preeclampsia. Galectin-7 impaired placentation,
535 elevated systolic blood pressure and induced albuminuria. Galectin-7 regulated
536 multiple pathways associated with the etiology of preeclampsia including the
537 renin-angiotensin system and sFlt-1.

538 **Figure Legends**

539 Figure 1. Galectin-7 was elevated in human chorionic villous samples (CVS) from pregnancies that
540 developed preterm preeclampsia. A. *LGALS7* expression in CVS. One-way ANOVA, $n=3-9$ /group.
541 B. Galectin-7 immunostaining in CVS (insert shows negative control) and quantification. One-way
542 ANOVA, $n=3-5$ /group. C. Galectin-7 (Gal7) treatment reduced first-trimester placental
543 trophoblast outgrowth (area within dotted line, normalized to length of outgrowth) compared to

544 vehicle control (Con). Paired t-test, $n=3$. D. *sFlt-1-e15a* and E. *sFlt-1* expression in first-trimester
545 placental villous cultured with galectin-7 or vehicle control. Student's t-test, $n=3-5$ /group. Data
546 presented as mean \pm SEM; * $P<0.05$. PPE, preterm preeclampsia; TPE, term preeclampsia; Un,
547 uncomplicated.

548

549 Figure 2. Galectin-7 administration (E8-12 or 5 day equivalent in non-pregnant [NP] mice) induced
550 hypertension and albuminuria in pregnant mice. A. systolic blood pressure (sBP). Mixed-effects
551 model (Sidak's multiple comparison test), $n=6-12$; B. Urinary albumin/creatinine ratio. Mixed-
552 effects model (Sidak's multiple comparison test), $n=5-10$; C. serum Flt-1 concentration. $n=3-6$; D.
553 Fetal and pup bodyweight. Two-way ANOVA (Sidak's multiple comparison test), $n=5-6$; E.
554 Placenta & decidua unit weight. Student's t-test, $n=4-6$; F. Fetal:placenta & decidua unit weight
555 ratio $n=4-6$. Data presented as mean \pm SEM; * $P<0.05$. E, embryonic day; P, post-natal day.

556

557 Figure 3. Galectin-7 administration (E8-12) dysregulated renin-angiotensin system (RAS) factor
558 production. A-D. RAS expression following galectin-7 administration in pregnant mice (E8-12) A.
559 *Agt* B. *Agtr1* C. *Renin* D. *Atp6a2* expression, Student's t-test, $n=3-6$. E&F. Angiotensinogen
560 production in human first-trimester placental villous cultured with galectin-7 (Gal7) or vehicle
561 control (Con) under 2% oxygen E. *Agt* expression F. Angiotensinogen secretion, Paired t-test,
562 $n=3$ /group. Data presented as mean \pm SEM; * $P<0.05$. E, embryonic day.

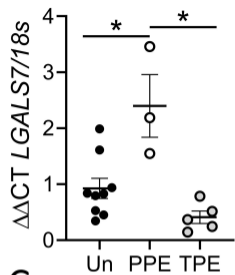
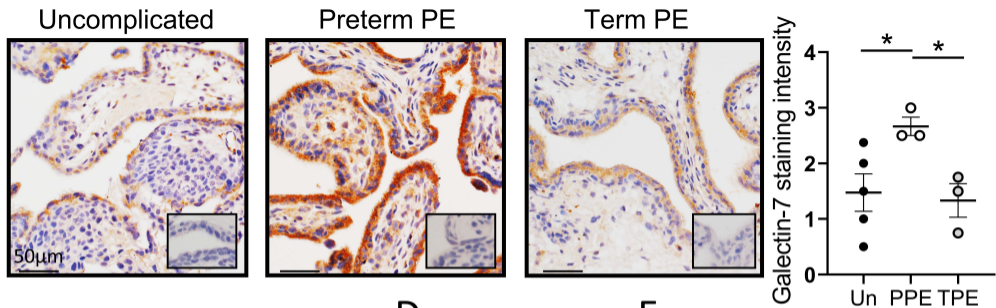
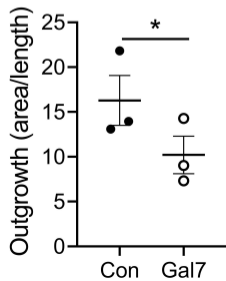
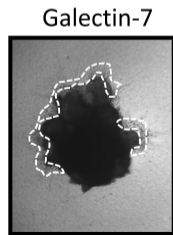
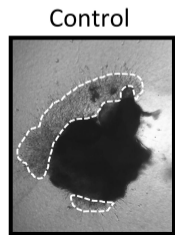
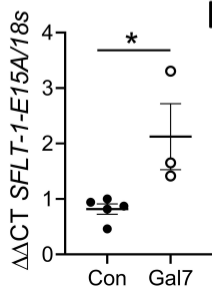
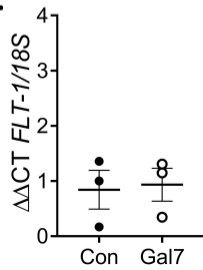
563

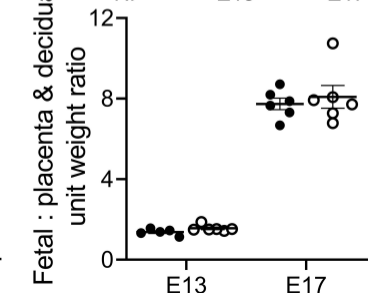
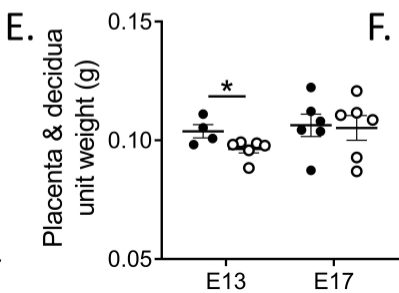
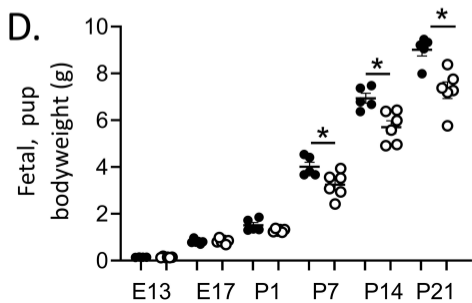
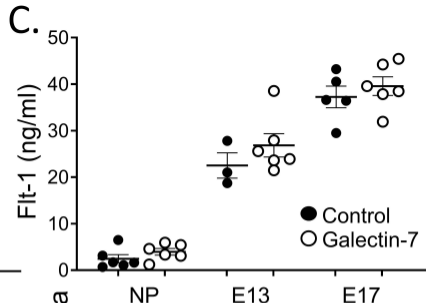
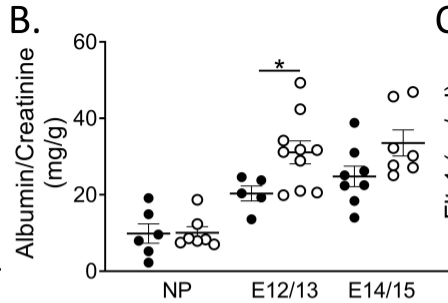
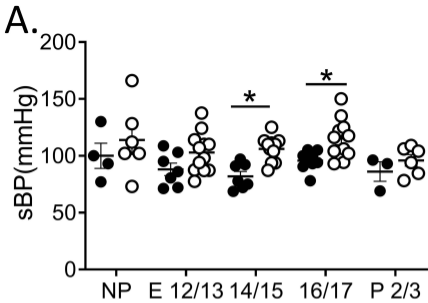
564 Figure 4. Galectin-7 administration (E8-12) impaired placental formation in mice. A.
565 Quantification of placental area: total, labyrinth, junctional, decidual and metrial lymphoid
566 aggregate of pregnancy (MLAp) zones at E13 and E17 of pregnancy. Student's t-test, $n=3-6$. B.
567 ISB4 staining in E13 and E17 placenta identifies placental zones. C. Fetal vascular branching (ISB4).
568 a is significantly different to b; Student's t-test, $n=5-6$; D. Trophoblast (cytokeratin; green)
569 invasion of decidual spiral arteries (α -SMA; red) in E13 implantation sites (Magnification 400x).
570 E. α -smooth muscle actin (α -SMA) surrounding E13 decidual spiral arteries. Student's t-test, $n=4-$
571 5. F. Decidual uterine Natural Killer (uNK) cells (DBA lectin) in E13 implantation sites. $n=5-6$. Data
572 presented as mean \pm SEM; * $P<0.05$. Insert shows negative control. E, embryonic day.

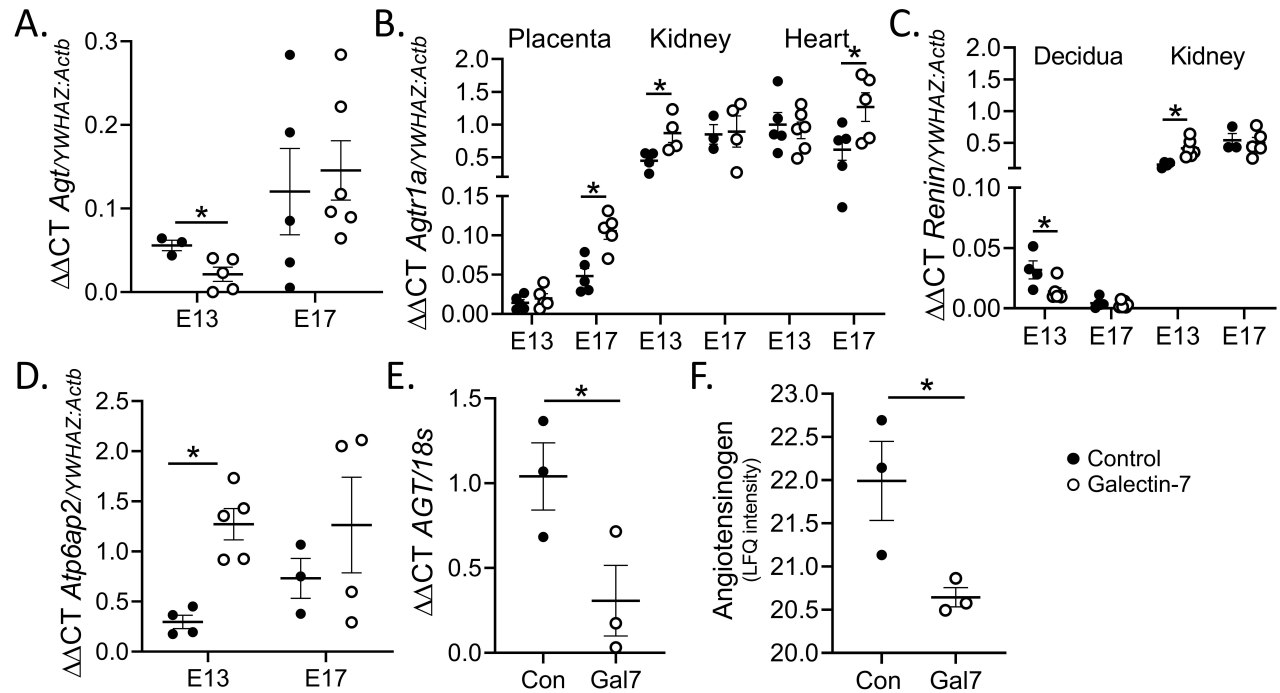
573 Figure 5. Galectin-7 administration (E8-12) altered mouse placental inflammatory cytokine
574 production. A. *IL1 β* B. *IL6* C. *IL10*. Student's t-test, $n=4-6$, Data presented as mean \pm SEM, * $P<0.05$.
575 E, embryonic day.

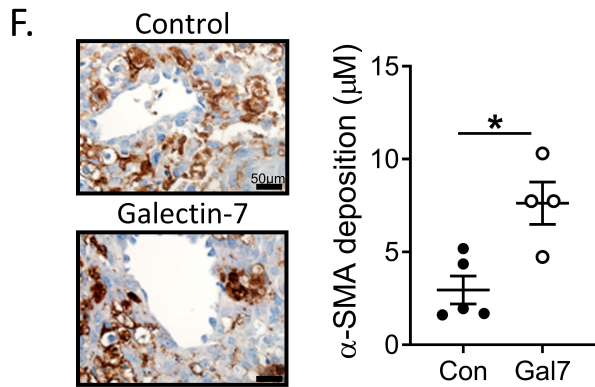
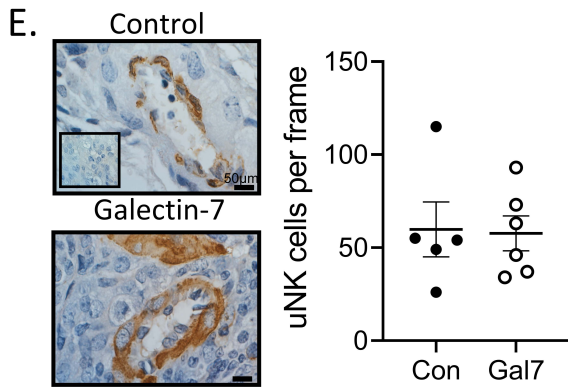
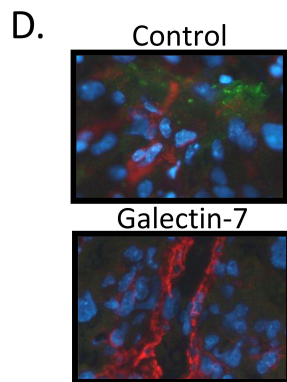
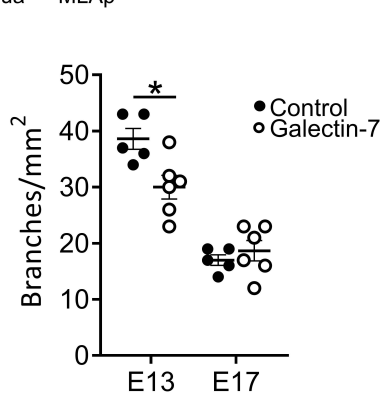
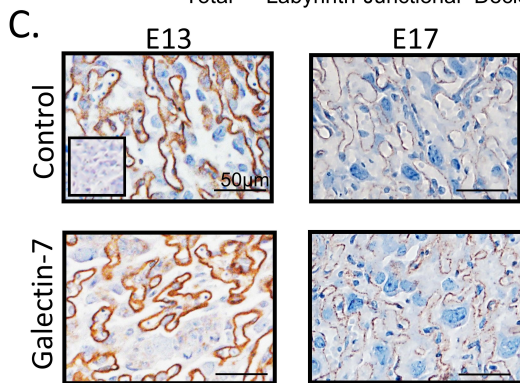
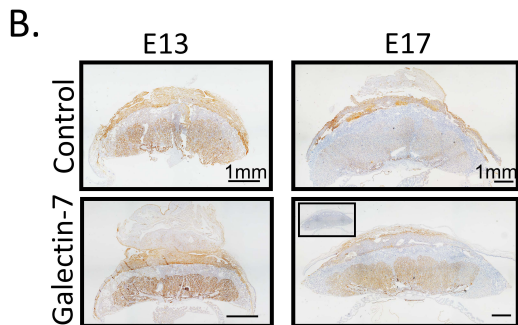
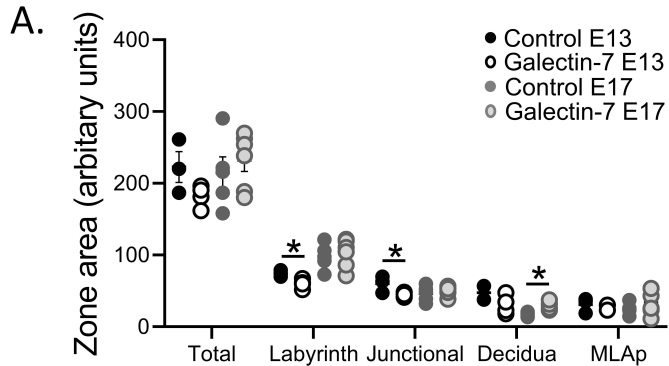
576 Figure 6. Galectin-7 treatment down-regulated ADAM12 production. A-D. First-trimester human
577 placental villous explants cultured with galectin-7 (Gal7) or vehicle control (Con) A. *MMP9*
578 expression. Paired t-test, $n=3$; B. *MMP9* protein secretion. Paired t-test, $n=4$. C. *ADAM12*
579 expression. Paired t-test, $n=3$. D. *ADAM12S* protein secretion. Paired t-test, $n=3$. E. *ADAM12*
580 expression in mouse placenta (Plac) and decidua (Dec) at E13. Student's t-test, $n=5-6$. F.
581 *ADAM12S* protein production in mouse placenta and decidua at E13. Student's t-test, $n=5-6$. Data
582 presented as mean \pm SEM; * $P<0.05$.

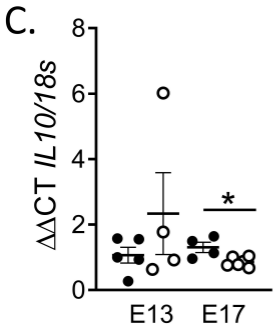
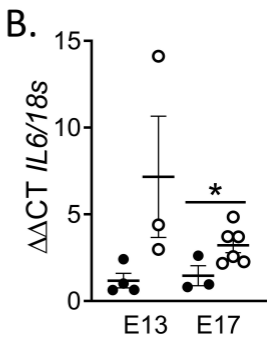
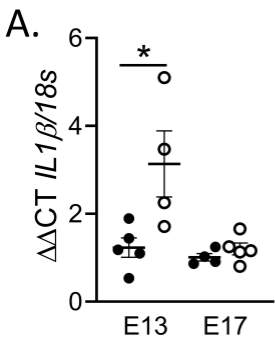
583

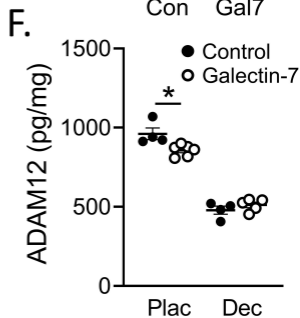
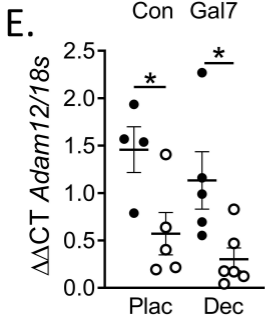
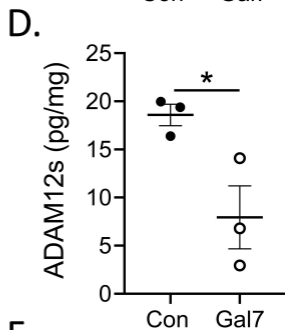
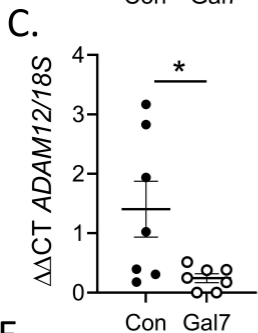
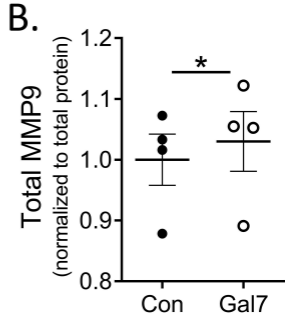
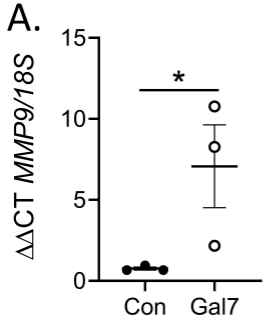
A.**B.****C.****D.****E.**











DATA SUPPLEMENT

Galectin-7 impairs placentation and causes preeclampsia features in mice

Ellen Menkhorst^{1,2,3,*}, Wei Zhou^{1,2}, Leilani Santos^{1,2}, Sarah Delforce^{4,5,6}, Teresa So^{1,2}, Kate Rainczuk³, Hannah Loke³, Argyro Syngelaki⁷, Swati Varshney⁸, Nicholas Williamson⁸, Kirsty Pringle^{4,5,6}, Morag J. Young^{9,10,^}, Kypros Nicolaides⁷, Yves St-Pierre¹¹, Eva Dimitriadis^{1,2,3,12,*}

¹Department of Obstetrics and Gynaecology, The University of Melbourne, Parkville, VIC, Australia

²Gynaecology Research Centre, Royal Women's Hospital, Parkville, VIC, Australia

³Centre for Reproductive Health, Hudson Institute of Medical Research, Clayton, VIC, Australia

⁴School of Biomedical Sciences and Pharmacy, University of Newcastle, Newcastle, NSW, Australia

⁵Priority Research Centre for Reproductive Sciences, University of Newcastle, Newcastle, NSW, Australia

⁶Pregnancy and Reproduction Program, Hunter Medical Research Institute, Newcastle, NSW, Australia

⁷Harris Birthright Research Centre for Fetal Medicine, King's College Hospital, London, United Kingdom

⁸Melbourne Mass Spectrometry and Proteomics Facility, Bio21 Molecular Science & Biotechnology Institute, The University of Melbourne, Melbourne, VIC, Australia

⁹Centre for Endocrinology and Metabolism, Hudson Institute of Medical Research, Clayton, VIC, Australia

¹⁰Baker Heart & Diabetes Institute, Prahran, VIC, Australia

¹¹INRS-Institut Armand-Frappier, Laval, QC, Canada

¹²Department of Anatomy and Developmental Biology, Monash University, Clayton, VIC, Australia

*Current address: ^{1,2}

^ Current address: ¹⁰

Short title: 50 characters

High placental galectin-7 precedes preeclampsia

Corresponding author: Eva Dimitriadis, Level 7, Royal Women's Hospital, 20 Flemington Rd, Parkville, VIC, Australia, 3052; Phone: +61 3 8345 2215; email: eva.dimitriadis@unimelb.edu.au

Supplementary methods:

Galectin-7 recombinant protein

Human galectin-7 recombinant protein from two sources were used in this project. Each batch was tested for activity (at concentrations recommended by the manufacturer) by determining the effect on the galectin-7 verified target MMP9 expression in human (primary trophoblast) and mouse cells (mouse kidney epithelial cell, TCMK1) by RT-qPCR and gelatin zymography. *Ex vivo* and *in vitro* primary first-trimester human villous cultures and outgrowth assays - R&D systems (#1339-GA; vehicle: 0.1% BSA in PBS); *in vivo* mouse experiments – R&D systems (pilot study; #1339-GA/CF; vehicle: PBS) and BioVision (#4647-1000; vehicle: PBS; Milpitas, CA USA).

Human placental tissue isolation and culture

Human placental tissue was collected under appropriate Human Research and Ethics Committee approvals (Monash Health and the Royal Women's Hospital, Melbourne #09317B; King's College Hospital, London REC:03-04-070). Written and informed consent was obtained from each patient before surgery.

Chorionic villous samples: Chorionic villous samples (CVS, n=20) taken from women undergoing screening for fetal chromosomal abnormalities were snap frozen immediately after collection. This patient cohort had no chromosomal abnormalities, was predominantly white (16/20), had spontaneous conception (19/20) and were all non-smokers. Further patient characteristics are shown in Tables S1&S2.

Placental and decidual tissue collection: First-trimester placental villous and decidua tissue was donated by healthy women undergoing pregnancy termination for psychosocial reasons (amenorrhea 6-12 weeks; n=82) and used for culture (n=11) or quantification of *Igals7* (qPCR)/galectin-7 (ELISA) across the first- and second-trimester.

Explant culture. Small pieces of first-trimester (amenorrhea 6-12 weeks) placental villous tissue (n=8) were dissected and cultured in DMEM/F-12 (containing 1% antibiotic/antimycotic) with 1µg/mL galectin-7 or vehicle control under 2% O₂, 5% CO₂ in a humidified chamber. Explants and conditioned media were collected after 16 and 72h respectively and snap frozen for RT-qPCR or mass spectrometry^{1, 2} as detailed in supplementary data.

Explant outgrowth assay. The effect of recombinant human galectin-7 on extravillous trophoblast outgrowth (n=3; amenorrhea 6-12 weeks) was measured and quantified using Motic Images Plus following 48h of treatment as previously described³. To account for differences in villous tip size and outgrowth potential, the outgrowth area was normalized to the length of villous from which the outgrowth occurred.

EVT isolation. Cytotrophoblast were isolated from first-trimester placental villous and cultured on Growth-factor Reduced Matrigel diluted 1:5 to promote differentiation to EVT phenotype as previously described⁴.

Recombinant galectin-7 administration

In vivo mouse experiments C57BL6 female (virgin 8-12 weeks) and male (8-52 weeks) mice (Monash Animal Services, Clayton VIC, Australia; WEHI, Kew, VIC, Australia) housed under conventional conditions, had ad libitum food and water and were maintained in a 12h: light-dark cycle. All procedures were approved by the Monash Medical Centre (B) (#MMCB2016/07) and Melbourne University (#1814697) Animal Ethics Committees. This study followed the NHMRC Australian Code of Practice for the Care and Use of Animals for Scientific Purposes.

Mice were haphazardly assigned to experimental groups. There was no allocation concealment or blinding of the experimenter who was required to give daily injections of the treatment/vehicle control, however for the primary outcome (hypertension) the actual blood pressure was calculated by a blinded assessor.

To determine the kinetics of galectin-7 serum clearance, 400µg/kg galectin-7 or vehicle control was injected subcutaneously to non-pregnant female mice before they were killed after 6, 16, 24 and 48 hours. Galectin-7 levels in serum peaked 24h after injection and were still detectable 48h after injection (Figure S3G).

To determine the effect of elevated galectin-7 on placental development and pregnancy outcome mated female mice received once daily sub-cutaneous injections of 400µg/kg/day galectin-7 or vehicle control from E8 (E, embryonic day; plug detection = E0) to E12, or for 5 consecutive days in non-pregnant mice. Pregnant mice were killed on E13 (n=5-6/group) E17 (n=6/group) or allowed to pup and the day of birth monitored. Pups were weighed on post-natal (P) days 1, 7, 14 and 21.

Serum and tissue collection Mice were killed by carbon dioxide inhalation followed by cardiac puncture to collect peripheral blood. Serum was separated by centrifugation at 500xg after 2h incubation at room temperature and snap-frozen. Implantation sites (≥ 5 /mouse) were dissected to obtain decidua/metrial lymphoid aggregate of pregnancy (MLAp), placenta and fetus. The placenta/decidua/MLAp were weighed as a single unit and fixed in 10% neutral buffered formalin or separated into placenta and decidua/MLAp and snap frozen on dry ice. The fetus was also weighed. For statistical analyses, placenta/decidua/MLAp or fetal weights from ≥ 3 - ≤ 5 implantation sites were averaged per dam. Tissues were subjected to gene array, RT-qPCR, ELISA, placental morphometry⁵, histology and immunohistochemistry as detailed in supplementary data.

Blood pressure measurements Systolic Blood Pressure (sBP) was measured in conscious pregnant mice every 2-3 days from E7 to day 2 following parturition (or corresponding days in non-pregnant mice) by tail-cuff plethysmography, following a procedure adapted from the manufacturer's manual (IITC Life Science), detailed previously³. Training prior to mating was not performed as pilot studies showed no benefit from this training, most likely as this occurred up to 3 weeks prior to the mouse becoming pregnant. Instead, mice were trained from E7-E11 in 2-3 sessions (or corresponding days in non-pregnant mice), before experimental readings were taken from E12 onwards.

Albuminuria Urine was collected opportunistically whenever mice were handled. Mice were scruffed over a clean plastic sheet and urine was collected if they urinated. Albumin/Creatinine levels in urine were determined using the Albuwell M and Creatinine companion kits (#1011 and 1012; Exocell) as per the manufacturer's instructions.

Gene expression

RNA was extracted from snap-frozen tissue using Tri Reagent (Sigma-Aldrich; Castle Hill, NSW, Australia) according to the manufacturer's instructions. Genomic DNA was digested using the DNAfree kit (Ambion, Thermo Scientific, Scoresby, Victoria, Australia) according to the manufacturer's instructions. RNA concentration, yield and purity were analyzed by spectrophotometry (Nanodrop Thermo Scientific, Scoresby, Victoria, Australia) at an absorbance ratio of A260/280nm.

PCR Array: To determine the mechanism by which the galectin-7 treated placenta induces the systemic features of PE we used a QIAGEN Preeclampsia Array (PAMM-163Z) as per the manufacturer's instructions on placental (Table S3), decidual (Table S4) and kidney (Table S5) tissues at E13 and E17. RNA was pooled from n=3 tissues for the array.

RT-qPCR: RNA was reverse transcribed using Superscript III First-Strand Synthesis System (Thermo-Fisher) according to the manufacturer's instructions except 0.5 μ L Superscript III was included per reaction. Real-time qPCR was performed using Power SYBR Green master mix (Applied Biosystems) on the ABI 7500HT or Veriti 7 fast block real-time qPCR systems (both Applied Biosystems) in duplicate or triplicate (final reaction volume, 10 μ l) in 96 or 384-well Micro Optical plates (Applied Biosystems). A template-free negative control in the presence of primers and RNase-free water only negative controls were added for each run. Primer sequences are shown in Tables S6 and S7; primers were obtained from Sigma-Aldrich. The qPCR protocol was as follows: 95 °C for 10 min and 40 cycles of 95 °C for 15s followed by 60°C for 1 min. Relative expression levels were calculated using comparative cycle threshold method ($\Delta\Delta$ CT) as outlined in the manufacturer's user manual.

ELISA

Galectin-7 (RayBio Technology human: ELH-Galectin7-1; mouse: ELM-Galectin7-1), ADAM12S (RayBio Technology human: ELH-ADAM12-1; Abcam mouse: ab213844), Flt-1 (R&D Systems mouse: MVR100) and Endoglin/CD105 (R&D Systems mouse: MNDG00) were assayed by ELISA as per the manufacturer's instructions.

ELISAs were performed on serum and cellular protein (ADAM12S human: 60 μ g/well; ADAM12 mouse: 50 μ g/well; Endoglin mouse: serum: diluted 1:4; Galectin-7 human: 60 μ g/well; Galectin-7 mouse: protein: 75 μ g/well, serum: diluted 1:4; Flt-1 mouse: serum: diluted 1:5) or conditioned media (100 μ l/well normalized to total cellular protein). Total protein was extracted from tissue by mechanical homogenization (QIAGEN Tissue Lyser) in Universal Lysis Buffer (50 mM Tris·HCl (pH 7.5), 150 mM NaCl, 2 mM EDTA, 2 mM EGTA, 25 mM NaF, 25 mM β -glycerolphosphate, protease inhibitor mixture [Calbiochem]), centrifuged at 10,000 \times g to pellet cell membrane and quantified using the BCA assay (Pierce).

Gelatin Zymography

Isolated EVT were treated with galectin-7 (1 μ g/ml) or control in DMEM/F12 media containing 1% antibiotic/antimycotic for 24h under 20% O₂, 5% CO₂ in a humidified chamber. Gelatinase activity in CM from isolated EVT was determined by zymography⁶. MMP9 bands were identified by comparison with molecular weight marker on each gel.

Mass spectrometry

Proteins in conditioned media from first-trimester placental villous (cultured with galectin-7/vehicle control for 72h under 2% O₂) were identified using mass spectrometry. 10 μ g total protein (quantified using BCA assay) was used for Solid-Phase Protein Preparation as previously described¹.

Sample Preparation: Proteins in conditioned media from first-trimester placental villous (cultured with galectin-7/vehicle control for 72h under 2% O₂) were identified using mass spectrometry. 10 μ g total protein (quantified using BCA assay) was used for Solid-Phase Protein Preparation as previously described^{1, 2}. Briefly, SP3 protocol was carried with 10 μ g of extracted protein samples in a total volume of 50 μ L Triethyl ammonium bicarbonate buffer (TEAB). These samples were subjected to reduction with 10 mM TCEP for 45 minutes at 37 °C followed by alkylation with 55 mM Iodoacetamide for 45 minutes at 37 °C in dark. Magnetic beads were prepared by combining 20 μ L of both, Sera-Mag Speed Beads A and B (GE Healthcare cat. no. 45152105050250; cat. no. 65152105050250) and washed two times with 200 μ L ddH₂O, and were re-suspend in 40 μ L ddH₂O for a final working concentration of 50 μ g/ μ L. 2 μ L of pre-washed magnetic beads as well as 50 μ L 100% ethanol were added to each sample. Protein binding to the beads was facilitated in ThermoMixer at 24 °C for 5 min at 1,000 r.p.m. After the binding is complete,

tubes were placed in a magnetic rack and were incubated until the beads have migrated to the tube wall. The supernatant was removed and beads were washed thrice with 180 μ L of 80% ethanol. Beads were resuspended in 100 μ L of 100 mM TEAB and sonicated for 5 minutes in a water bath. The samples were then kept for overnight digestion at 37°C and 1000 rpm in a table-top thermomixer after adding sequencing-grade trypsin in an enzyme:protein ratio of 1:10. Upon digestion, peptides were recovered by collecting the supernatant. These peptides were lyophilized and stored until mass analysis.

LC-MS/MS analysis: Lastly for subsequent LC-MS/MS analysis, samples were reconstituted in 30 μ L 2% acetonitrile:0.1% trifluoroacetic acid and were analysed on a LTQ Orbitrap Elite (Thermo Scientific) coupled to an Ultimate 3000 RSLC nanosystem (Dionex). The nanoLC system was equipped with an Acclaim Pepmap nano-trap column and an Acclaim Pepmap analytical column. 6 μ L of the peptide mix was loaded onto the trap column at 3% CH₃CN containing 0.1% formic acid for 5 min before the enrichment column is switched in-line with the analytical column. The LC gradient used was 3% B to 20% B for 95 min, 20% B to 40% B in 10 min, 40% B to 80% B in 5 min and maintained at 80% B for the final 5 min before equilibration for 10 min at 3% B prior to the next analysis. The LTQ Orbitrap Elite mass spectrometer was operated in the data-dependent mode, spectra acquired first in positive mode at 240k resolution followed by collision induced dissociation (CID) fragmentation. Twenty of the most intense peptide ions with charge states ≥ 2 were isolated and fragmented using normalized collision energy of 35 and activation Q of 0.25 (CID).

Data Analysis: Raw data files were searched against the Human protein reference proteomes (UniProt Proteome ID: [UP000005640](#)) using MaxQuant-Andromeda (version 1.6.7.0). The false discovery rate (FDR) was set at 0.01 for both peptides and proteins. Search parameters were set as follows: variable modifications: Oxidation (M), Acetyl (Protein N-term); fixed modifications: cysteine carbamidomethylation. The analysis of the samples was based on the label-free quantification (LFQ) intensities. The data was statistically evaluated using Perseus software (version 1.6.7.0). The protein data was filtered categorically by row for reverse identifications (false positives), contaminants, and proteins “only identified by site”. The fold changes in the protein levels were evaluated by comparing the mean LFQ intensities amid all experimental groups. A protein was considered to be differentially expressed if the difference was statistically significant ($p < 0.05$), the fold change >1.2 and < 0.88 was identified with a minimum of 2 peptides.

Histology and Immunohistochemistry

Monash Histology Platform (Monash University) and Laboratory Services (Royal Children’s Hospital) processed and sectioned all formalin fixed tissues and performed histological staining as required (Hematoxylin and eosin, Periodic Acid Schiff and Masson’s trichrome).

CVS: Snap-frozen CVS were fixed in 10% formalin at 4°C for 20h, washed 3x with Tris buffered saline (TBS) before processing and embedding in paraffin, sectioned at 4 μ m, placed onto SuperFrost slides, dried, deparaffinized, and rehydrated. Immunostaining for galectin-7 was performed as previously described⁷ except the primary antibody (AF1339, R&D Systems) concentration was 0.67 μ g/ml. Two runs were performed with a quality control included in each run. Immunostaining intensity in the syncytiotrophoblast was assessed (0, no staining to 3, intense staining) by a blinded scorer for each run (different scorer each run) and the values for the two runs averaged to give an intensity score for each tissue.

Mouse tissues: Fresh placenta/decidua was fixed in 10% formalin at 4°C, washed 2x with TBS before processing and embedding in paraffin, sectioning at 5 μ m, before being placed onto SuperFrost slides, dried, deparaffinized, and rehydrated.

DBA lectin (Vector Laboratories) and isolectin B4 (ISB4; Sigma) staining were performed as per the manufacturer's instructions to highlight decidual uNK cells and the extracellular matrix surrounding fetal blood vessels, respectively.

For immunohistochemical analysis antibodies against α -SMA (IHC: 1:100 dilution; M0851, clone 1A4; Dako), galectin-7 (0.444 μ g/ml, AF1339, R&D Systems) and desmin (0.4 μ g/ml, D93F5, Cell Signaling Technology) were used. α -SMA IHC was performed using the Vector M.O.M kit (Vector Laboratories), including antigen retrieval using EDTA buffer. For galectin-7 staining antigen retrieval was performed using 0.01M Citrate buffer. For galectin-7 and desmin staining peroxidase activity was blocked by incubation with 3% hydrogen peroxidase. Primary antibody or isotype negative control goat/rabbit IgG in blocking solution were applied for 18h incubated at 4°C. After stringent washing with 0.6% Tween-20 in TBS, antibody localization was detected by sequential application of biotinylated horse anti-goat (galectin-7) or goat-anti rabbit (desmin) IgG (1:200; Vector Laboratories) in blocking solution for 30 min and in an avidin-biotin complex conjugated to horseradish peroxidase (HRP) (Vector Laboratories). Protein was visualized as a brown precipitate using diaminobenzidine tetrahydrochloride substrate (Dako). Sections were counterstained with Harris hematoxylin (Sigma Chemicals) and mounted.

For immunofluorescence, formalin-fixed sections were treated as described above, except that antigen retrieval was performed using EDTA buffer; CAS block and non-immune serum was diluted in and washes were performed in PBS; primary antibody for pan cytokeratin (5 μ g/ml, sc-H-240; Santa Cruz Biotechnology), α -SMA (1:200 dilution; M0851, clone 1A4; Dako) or non-immune goat IgG (isotype negative control) were applied, followed by secondary antibody incubation (Donkey α -mouse alexa fluor 488 and Donkey α -goat alexa fluor 594; both 1:200) in non-immune serum for 2 h at room temperature; and following further washes, sections were mounted using Vectastain containing DAPI (DAKO).

Placental Morphometry

Histology images are of mid-sagittal sections from hemisected implantation sites. All placental morphometry was quantified using Image J⁵ or Cellsense software and performed on three separate fields of view. One placenta per mouse was analyzed and data collected from one section per placenta.

To determine the area of each placental/decidual zone, digital photographs were taken at 4x magnification and stitched together using CellSense software to create one image. Placental/decidua stained with ISB4 and desmin were used to define labyrinth, junctional, decidual and MLAp zones⁸. The area of each zone was quantified using Image J software⁵.

To assay vessel density vessels stained with ISB4 in the middle region of the labyrinth were counted using Image J software.

To assay smooth muscle cells around decidual arteries Image J software was used to measure smooth muscle layer thickness (perpendicular to artery wall) in all vessels visible in the frame (minimum of 3 vessels per frame) as identified by α -SMA staining.

CellSense software was used to quantify DAB staining in the decidua (uNK cell number), expressed as cell number per frame.

Statistics

Statistical analyses were performed by GraphPad Prism version 8.3.1. $P < 0.05$ was considered significant. Data were tested for normality and statistical tests (indicated in figure legends) chosen according to experimental design. A two-sided P value was calculated for all experiments.

Supplemental References:

1. Dagley LF, Infusini G, Larsen RH, Sandow JJ, Webb AI. Universal solid-phase protein preparation (usp3) for bottom-up and top-down proteomics. *Journal of Proteome Research*. 2019;18:2915-2924
2. Hughes CS, Moggridge S, Müller T, Sorensen PH, Morin GB, Krijgsveld J. Single-pot, solid-phase-enhanced sample preparation for proteomics experiments. *Nature Protocols*. 2019;14:68-85
3. Winship AL, Koga K, Menkhorst E, Van Sinderen M, Rainczuk K, Nagai M, Cuman C, Yap J, Zhang J-G, Simmons D, Young MJ, Dimitriadis E. Interleukin-11 alters placentation and causes preeclampsia features in mice. *PNAS*. 2015;112:15928-15933
4. Menkhorst EM, Lane N, Winship A, Li P, Yap J, Meehan K, Rainczuk A, Stephens AN, Dimitriadis E. Decidual-secreted factors alter invasive trophoblast membrane and secreted proteins implying a role for decidual cell regulation of placentation. *PLoS ONE*. 2012;7:e31418
5. Garcia-Gonzalez MA, Outeda P, Zhou Q, Zhou F, Menezes LF, Qian F, Huso DL, Germino GG, Piontek KB, Watnick T. Pkd1 and pkd2 are required for normal placental development. *PLoS ONE*. 2010;5:e12821
6. Paiva P, Salamonsen LA, Manuelpillai U, Dimitriadis E. Interleukin 11 inhibits human trophoblast invasion indicating a likely role in the decidual restraint of trophoblast invasion during placentation. *BOR*. 2009;80:302-210
7. Menkhorst EM, Gamage T, Cuman C, Kaitu'u-Lino TuJ, Tong S, Dimitriadis E. Galectin-7 acts as an adhesion molecule during implantation and increased expression is associated with miscarriage. *Placenta*. 2014;35:195-201
8. Edwards AK, Janzen-Pang J, Peng A, Tayade C, Carniata A, Yamada A, Lima P, Tse. Microscopic anatomy of the pregnant mouse uterus during gestation. In: Croy BA, Yamada AT, DeMayo FJ, Adamson SL, eds. *The guide to the investigation of mouse pregnancy*. Academic Press; 2014:43-67.

Supplemental Table S1**Patient characteristics of women providing Chorionic Villous Samples for *LGALS7* RT-qPCR.**

Characteristic	Normotensive (n=9)	Preterm preeclampsia (n=3)	Term preeclampsia (n=6)	P value (*,<0.05)
Maternal age (years)	34.6 (28.7-41.2)	35.2 (30.0-44.9)	35.9 (29.0-44.1)	0.9389
Maternal BMI (kg/m ²)	23.7 (21.5-28.4)	22.7 (18.1-31.4)	24.7 (23.7-29.9)	0.7851
Previous pregnancies	9 Multiparous-no PE	1 Nulliparous, 2 Multiparous- no PE	3 Nulliparous, 2 multiparous-no PE	
Gestational age of CVS (weeks)	13.1 (12.1-14.6)	12.6 (12.3-12.7)	12.5 (12.2-13.5)	0.6140
Gestational age of delivery (weeks)	40.2 (38.4-41.0)	35.2 (30.9-35.4)	39.6 (37.9-40.9)	<0.0001*
Birth weight (grams)	3700 (3193-3866)	2298 (895-2432)	2946 (2455-3398)	0.0005*
Neonatal gender (male)	4 (50%)	3 (100%)	1 (16.7%)	

Data presented as median (interquartile range) or n (%); statistics: One-way ANOVA.

Supplemental Table S2**Patient characteristics of women providing Chorionic Villous Samples for galectin-7 IHC.**

Characteristic	Normotensive (n=5)	Preterm preeclampsia (n=3)	Term preeclampsia (n=3)	P value (*,<0.05)
Maternal age (years)	31.7 (27.8-37.9)	35.2 (30.0-44.9)	30.1 (25.7-36.3)	0.7061
Maternal BMI (kg/m ²)	21.6 (20.1-28.5)	22.7 (18.1-31.4)	28.4 (24.2-34.2)	0.3997
Previous pregnancies	5 Multiparous-no PE	1 Nulliparous, 2 Multiparous- no PE	3 Nulliparous	
Gestational age of CVS (weeks)	12.1 (11.9-13.6)	12.6 (12.3-12.7)	12.4 (11.6-13.4)	0.9763
Gestational age of delivery (weeks)	40.0 (38.0-41.0)	35.2 (30.9-35.4)	40.8 (37.7-41.0)	<0.0074*
Birth weight (grams)	3462 (2895-3790)	2298 (895-2432)	3320 (2327-3632)	0.0354*
Neonatal gender (male)	2 (40)	3 (100)	0 (0)	

Data presented as median (interquartile range) or n (%); statistics: One-way ANOVA.

Supplemental Table S3

Fold-change in Preeclampsia Array gene expression: pooled (n=3) placental tissue

		E13 PBS	E13 Galectin-7		E17 PBS	E17 Galectin-7	
Well	Gene	2 [^] (-Avg.(Delta(Ct)))		Fold Change	2 [^] (-Avg.(Delta(Ct)))		Fold Change
A01	<i>Abcc1</i>	0.000216	0.000216	1.0005	0.000192	0.000221	1.1523
A02	<i>Abcg2</i>	1.928382	0.510193	0.2646	0.50566	0.319659	0.6322
A03	<i>Adm</i>	2.723173	1.172672	0.4306	2.18704	1.048577	0.4795
A04	<i>Agtr1a</i>	0.251479	0.307825	1.2241	0.533823	0.669577	1.2543
A05	<i>Angpt2</i>	5.57627	4.125438	0.7398	4.038617	2.83267	0.7014
A06	<i>Apln</i>	0.629422	0.244808	0.3889	0.355971	0.36503	1.0254
A07	<i>Atp1b1</i>	10.058083	11.526912	1.146	14.538226	15.617618	1.0742
A08	<i>Atp2a2</i>	6.276871	5.722693	0.9117	6.195	5.224929	0.8434
A09	<i>Bcl6</i>	0.757339	0.545579	0.7204	0.953165	0.375441	0.3939
A10	<i>Bhlhe40</i>	1.149699	2.014073	1.7518	2.285959	2.53269	1.1079
A11	<i>C3</i>	2.095647	4.149922	1.9803	0.953778	0.640478	0.6715
A12	<i>Cav1</i>	0.921796	0.92301	1.0013	1.267609	2.017905	1.5919
B01	<i>Ccl12</i>	0.152035	0.064364	0.4233	0.104914	0.129335	1.2328
B02	<i>Cd40lg</i>	0.000216	0.000216	1.0005	0.001449	0.004183	2.8874
B03	<i>Cdh13</i>	1.767718	0.555378	0.3142	0.937993	1.05802	1.128
B04	<i>Cfd</i>	0.005197	0.0119	2.2899	0.009996	0.004087	0.4088
B05	<i>Clu</i>	2.714833	2.862973	1.0546	4.640021	7.767819	1.6741
B06	<i>Col14a1</i>	0.922925	0.292596	0.317	0.188018	0.342037	1.8192
B07	<i>Cp</i>	0.58059	0.241729	0.4163	0.000192	0.904054	4706.4325
B08	<i>Crh</i>	0.029507	0.008904	0.3017	0.004189	0.002054	0.4903
B09	<i>Crhbp</i>	0.000216	0.007305	33.7786	0.024969	0.004435	0.1776
B10	<i>Cxcl10</i>	0.075627	0.074457	0.9845	0.060755	0.062316	1.0257
B11	<i>Cxcl9</i>	0.171271	0.000216	0.0013	0.000192	0.000221	1.1523
B12	<i>Cxcr4</i>	0.234896	0.272804	1.1614	0.196746	0.271819	1.3816
C01	<i>Cyp26a1</i>	0.008781	0.029277	3.334	0.011377	0.006538	0.5747
C02	<i>Dcn</i>	35.447415	30.929255	0.8725	66.753118	79.287444	1.1878

C03	<i>Dusp1</i>	3.013925	3.971831	1.3178	4.046255	3.432699	0.8484
C04	<i>Edn1</i>	0.90572	0.160181	0.1769	0.299944	0.271181	0.9041
C05	<i>Eng</i>	1.132504	1.476609	1.3038	1.004304	0.688918	0.686
C06	<i>F5</i>	0.15535	0.099904	0.6431	0.039136	0.071764	1.8337
C07	<i>Fabp4</i>	15.52781	15.023762	0.9675	19.06452	16.37949	0.8592
C08	<i>Flt1</i>	1.622373	1.985183	1.2236	2.072477	1.53162	0.739
C09	<i>Flt4</i>	1.198594	1.250613	1.0434	2.127983	1.288873	0.6057
C10	<i>Fstl3</i>	7.435535	0.7966	0.1071	5.786249	3.013854	0.5209
C11	<i>H2-M3</i>	0.267123	0.459792	1.7213	0.666392	0.622688	0.9344
C12	<i>Hbegf</i>	1.025066	0.680375	0.6637	0.933311	0.60879	0.6523
D01	<i>Hgf</i>	0.035341	0.02471	0.6992	0.04794	0.079497	1.6583
D02	<i>Hif1a</i>	5.917179	6.081445	1.0278	7.361646	7.176859	0.9749
D03	<i>Hp</i>	0.106006	0.068534	0.6465	0.056956	0.093547	1.6424
D04	<i>Hsd17b1</i>	0.000216	0.005245	24.2548	0.004367	0.002398	0.5491
D05	<i>Hsp90aa1</i>	55.466374	27.795168	0.5011	32.752572	18.003425	0.5497
D06	<i>Htr3a</i>	0.000216	0.000216	1.0005	0.000192	0.000221	1.1523
D07	<i>Htra1</i>	4.980534	6.528865	1.3109	14.046466	13.28595	0.9459
D08	<i>Ifng</i>	0.001182	0.000216	0.1831	0.006496	0.000221	0.0341
D09	<i>Igf1</i>	0.061235	0.05642	0.9214	0.120639	0.123256	1.0217
D10	<i>Igfbp3</i>	2.752208	3.440407	1.2501	3.853307	6.224576	1.6154
D11	<i>Il10</i>	0.002816	0.005933	2.107	0.001072	0.001904	1.7767
D12	<i>Il11</i>	0.003814	0.000216	0.0567	0.002578	0.001091	0.4231
E01	<i>Il15</i>	0.123681	0.065299	0.528	0.111887	0.172872	1.5451
E02	<i>Il18</i>	0.088554	0.05464	0.617	0.035661	0.065147	1.8268
E03	<i>Il1a</i>	0.186756	0.391174	2.0946	0.266213	0.156877	0.5893
E04	<i>Il2</i>	0.000216	0.000216	1.0005	0.000192	0.001824	9.4931
E05	<i>Il6</i>	0.059487	0.018741	0.315	0.016698	0.01933	1.1577
E06	<i>Inha</i>	0.086866	0.114292	1.3157	0.1573	0.235971	1.5001
E07	<i>Inhba</i>	3.130998	1.843474	0.5888	30.261956	13.975796	0.4618
E08	<i>Itgb3</i>	7.219168	8.713233	1.207	21.830849	14.458696	0.6623
E09	<i>Kit</i>	4.130898	4.062498	0.9834	8.147494	10.043537	1.2327

E10	<i>Krt19</i>	55.735148	24.643345	0.4422	83.461059	40.280272	0.4826
E11	<i>Lep</i>	0.0003	0.000216	0.7218	0.000702	0.000221	0.3154
E12	<i>Lpl</i>	2.052035	0.903232	0.4402	1.371981	1.438655	1.0486
F01	<i>Mas1</i>	0.073779	0.046313	0.6277	0.099789	0.115341	1.1558
F02	<i>Mmp12</i>	0.234462	0.503466	2.1473	1.164057	0.780371	0.6704
F03	<i>Mmp9</i>	0.059527	0.037383	0.628	0.111145	0.042716	0.3843
F04	<i>Ncam1</i>	1.672422	2.224819	1.3303	3.179772	1.484134	0.4667
F05	<i>Ndrp1</i>	7.423788	12.76297	1.7192	14.79679	22.05874	1.4908
F06	<i>Nos3</i>	0.024096	0.075557	3.1356	0.030264	0.066753	2.2057
F07	<i>Ntrk2</i>	0.102704	0.087713	0.854	0.165224	0.30539	1.8483
F08	<i>Pappa2</i>	84.049976	86.931202	1.0343	118.248684	93.656908	0.792
F09	<i>Pdgfd</i>	0.066554	0.234646	3.5257	0.161048	0.331163	2.0563
F10	<i>Pgf</i>	1.702277	2.344214	1.3771	3.107625	2.961064	0.9528
F11	<i>Pgr</i>	1.986124	1.164195	0.5862	1.615204	1.45754	0.9024
F12	<i>Qpct</i>	9.239498	4.374203	0.4734	5.218356	5.556034	1.0647
G01	<i>Serpina3n</i>	0.24147	0.303966	1.2588	0.490854	0.364062	0.7417
G02	<i>Sod1</i>	20.722419	10.475217	0.5055	12.266088	10.86986	0.8862
G03	<i>Spp1</i>	18.904588	13.583527	0.7185	12.29474	5.55848	0.4521
G04	<i>Stat1</i>	4.804278	5.684148	1.1831	3.946253	2.986454	0.7568
G05	<i>Tac1</i>	2.129389	0.06466	0.0304	0.000192	0.075275	391.8735
G06	<i>Tac2</i>	0.031599	0.033326	1.0547	0.068441	0.035092	0.5127
G07	<i>Tek</i>	0.393273	0.575852	1.4643	0.676445	0.882153	1.3041
G08	<i>Tgfb1</i>	4.076258	3.670504	0.9005	2.522628	4.184095	1.6586
G09	<i>Tnf</i>	0.01848	0.044533	2.4098	0.078123	0.143867	1.8415
G10	<i>Trem1</i>	0.020765	0.03994	1.9234	0.020794	0.013661	0.657
G11	<i>Vcan</i>	0.195159	0.401375	2.0567	1.057582	1.447746	1.3689
G12	<i>Vegfa</i>	1.414476	4.200451	2.9696	5.531291	7.996283	1.4456
H01	<i>Actb</i>	192.961538	173.62263	0.8998	79.399241	150.825077	1.8996
H02	<i>B2m</i>	80.654745	84.462801	1.0472	100.760007	87.576356	0.8692
H03	<i>Gapdh</i>	78.373037	67.093318	0.8561	59.038343	50.215802	0.8506
H04	<i>Gusb</i>	0.940999	0.894052	0.9501	1.051905	0.959303	0.912

H05	<i>Hsp90ab1</i>	45.210485	40.882349	0.9043	18.096808	28.783548	1.5905
H06	<i>MGDC</i>	0.000401	0.000216	0.5396	0.000233	0.000221	0.9488
H07	<i>RTC</i>	23.400339	21.183017	0.9052	18.519989	24.52254	1.3241
H08	<i>RTC</i>	25.358113	22.949204	0.905	23.509946	82.665446	3.5162
H09	<i>RTC</i>	22.5769	21.318606	0.9443	21.712837	22.471905	1.035
H10	<i>PPC</i>	101.601613	76.135172	0.7494	70.177192	78.050475	1.1122
H11	<i>PPC</i>	93.300215	80.249316	0.8601	99.256544	86.86352	0.8751
H12	<i>PPC</i>	461.605467	63.521857	0.1376	74.720868	84.567446	1.1318

Supplemental Table S4

Fold-change in Preeclampsia Array gene expression: pooled (n=3) decidual tissue

		E13 PBS	E13 Galectin-7		E17 PBS	E17 Galectin-7	
Well	Gene	2 ^{^(-Avg.(Delta(Ct)))}		Fold Change	2 ^{^(-Avg.(Delta(Ct)))}		Fold Change
A01	<i>Abcc1</i>	0.000011	0.000012	1.1123	0.000011	0.000012	1.0754
A02	<i>Abcg2</i>	0.21388	0.034206	0.1599	0.025705	0.024279	0.9445
A03	<i>Adm</i>	0.692815	0.223858	0.3231	0.47795	0.192563	0.4029
A04	<i>Agtr1a</i>	0.001061	0.00463	4.3645	0.008011	0.060247	7.5203
A05	<i>Angpt2</i>	0.433507	0.291785	0.6731	0.198021	0.036614	0.1849
A06	<i>Apln</i>	0.036275	0.022025	0.6072	0.012231	0.016562	1.3542
A07	<i>Atp1b1</i>	0.337736	0.38062	1.127	0.243878	0.262664	1.077
A08	<i>Atp2a2</i>	0.556428	0.481661	0.8656	0.368743	0.504025	1.3669
A09	<i>Bcl6</i>	0.023269	0.024104	1.0359	0.033252	0.028098	0.845
A10	<i>Bhlhe40</i>	0.406991	0.25896	0.6363	0.238634	0.13854	0.5806
A11	<i>C3</i>	2.83755	2.609678	0.9197	4.822191	4.718803	0.9786
A12	<i>Cav1</i>	0.227722	0.288732	1.2679	0.202077	0.294135	1.4556
B01	<i>Ccl12</i>	0.081587	0.02633	0.3227	0.016243	0.031285	1.9261
B02	<i>Cd40lg</i>	0.000011	0.000012	1.0968	0.000146	0.00018	1.2345
B03	<i>Cdh13</i>	0.093916	0.053123	0.5656	0.10691	0.068721	0.6428
B04	<i>Cfd</i>	0.000011	0.000591	53.2436	0.001195	0.000849	0.7108
B05	<i>Clu</i>	0.103393	0.064134	0.6203	0.107805	0.300635	2.7887
B06	<i>Col14a1</i>	0.013547	0.325613	24.0359	0.024192	0.051828	2.1424
B07	<i>Cp</i>	0.031135	0.016848	0.5411	0.042261	0.284314	6.7275
B08	<i>Crh</i>	0.000889	0.000063	0.0707	0.000011	0.000012	1.0754
B09	<i>Crhbp</i>	0.000011	0.00023	20.6692	0.000343	0.000301	0.8754
B10	<i>Cxcl10</i>	0.019364	0.035796	1.8486	0.018209	0.014792	0.8124
B11	<i>Cxcl9</i>	0.001322	0.0021	1.5885	0.000586	0.001618	2.7594
B12	<i>Cxcr4</i>	0.012181	0.009553	0.7843	0.008207	0.011961	1.4574

C01	<i>Cyp26a1</i>	0.018205	0.009458	0.5195	0.019112	0.021734	1.1372
C02	<i>Dcn</i>	9.347674	10.745465	1.1495	11.549719	13.731545	1.1889
C03	<i>Dusp1</i>	0.206254	0.2296	1.1132	0.359462	0.264079	0.7347
C04	<i>Edn1</i>	0.048834	0.011597	0.2375	0.016401	0.019793	1.2069
C05	<i>Eng</i>	0.119204	0.137645	1.1547	0.083415	0.0577	0.6917
C06	<i>F5</i>	0.009338	0.012115	1.2974	0.014726	0.035506	2.4111
C07	<i>Fabp4</i>	3.043562	3.945448	1.2963	1.288638	0.792469	0.615
C08	<i>Flt1</i>	0.028278	0.015663	0.5539	0.060374	0.038913	0.6445
C09	<i>Flt4</i>	0.118878	0.124486	1.0472	0.157542	0.124295	0.789
C10	<i>Fstl3</i>	0.047756	0.025763	0.5395	0.037841	0.015338	0.4053
C11	<i>H2-M3</i>	0.044919	0.058316	1.2983	0.062147	0.06601	1.0622
C12	<i>Hbegf</i>	0.032321	0.02578	0.7976	0.041918	0.013891	0.3314
D01	<i>Hgf</i>	0.014592	0.015225	1.0434	0.007463	0.012567	1.6839
D02	<i>Hif1a</i>	0.302734	0.272931	0.9016	0.273255	0.292294	1.0697
D03	<i>Hp</i>	0.0139	0.011522	0.8289	0.028273	0.03537	1.251
D04	<i>Hsd17b1</i>	0.000381	0.000616	1.6152	0.000397	0.00162	4.0809
D05	<i>Hsp90aa1</i>	0.559315	0.706479	1.2631	0.870316	0.512365	0.5887
D06	<i>Htr3a</i>	0.000034	0.000017	0.4904	0.000011	0.000012	1.0754
D07	<i>Htra1</i>	0.5155	0.058177	0.1129	0.126885	0.286613	2.2588
D08	<i>Ifng</i>	0.000582	0.000327	0.5622	0.001109	0.002084	1.879
D09	<i>Igf1</i>	0.023205	0.031877	1.3737	0.022775	0.05095	2.2371
D10	<i>Igfbp3</i>	0.379582	0.166533	0.4387	0.313814	0.457576	1.4581
D11	<i>Il10</i>	0.000601	0.000267	0.4436	0.000292	0.000255	0.8718
D12	<i>Il11</i>	0.000634	0.000552	0.871	0.000884	0.000395	0.4473
E01	<i>Il15</i>	0.017086	0.027957	1.6362	0.015155	0.020648	1.3624
E02	<i>Il18</i>	0.006582	0.00508	0.7718	0.007956	0.009886	1.2426
E03	<i>Il1a</i>	0.052838	0.019134	0.3621	0.061817	0.0406	0.6568
E04	<i>Il2</i>	0.000011	0.000012	1.1123	0.000011	0.000012	1.0754
E05	<i>Il6</i>	0.007109	0.000828	0.1164	0.002009	0.001046	0.5207
E06	<i>Inha</i>	0.001935	0.005549	2.867	0.006155	0.004262	0.6925
E07	<i>Inhba</i>	0.216171	0.208957	0.9666	5.386275	1.66197	0.3086

E08	<i>Itgb3</i>	0.656052	0.697241	1.0628	0.898934	0.78191	0.8698
E09	<i>Kit</i>	0.18684	0.176411	0.9442	0.362771	0.15259	0.4206
E10	<i>Krt19</i>	0.250113	0.169299	0.6769	0.489995	4.294937	8.7653
E11	<i>Lep</i>	0.000011	0.000012	1.1123	0.000011	0.000013	1.2162
E12	<i>Lpl</i>	0.027928	0.034006	1.2176	0.26054	0.485441	1.8632
F01	<i>Mas1</i>	0.003274	0.00259	0.7911	0.004604	0.003925	0.8526
F02	<i>Mmp12</i>	0.008448	0.004875	0.5771	0.055204	0.027718	0.5021
F03	<i>Mmp9</i>	0.005562	0.007497	1.3478	0.009475	0.009251	0.9764
F04	<i>Ncam1</i>	0.049434	0.025798	0.5219	0.093482	0.223774	2.3938
F05	<i>Ndr1</i>	0.574561	0.612041	1.0652	0.910893	0.400581	0.4398
F06	<i>Nos3</i>	0.004909	0.012318	2.5092	0.007322	0.009308	1.2712
F07	<i>Ntrk2</i>	0.077875	0.129625	1.6645	0.096775	0.107629	1.1122
F08	<i>Pappa2</i>	1.314201	0.503777	0.3833	3.28448	1.893013	0.5764
F09	<i>Pdgfd</i>	0.016099	0.028191	1.7511	0.034894	0.04613	1.322
F10	<i>Pgf</i>	0.30615	0.083558	0.2729	0.267879	0.214607	0.8011
F11	<i>Pgr</i>	0.70071	0.625802	0.8931	0.407139	0.531939	1.3065
F12	<i>Qpct</i>	0.642421	0.666873	1.0381	0.804472	0.576555	0.7167
G01	<i>Serpina3n</i>	0.104768	0.163829	1.5637	0.043272	0.107137	2.4759
G02	<i>Sod1</i>	0.53502	0.44527	0.8322	0.523494	0.518651	0.9907
G03	<i>Spp1</i>	12.492947	13.29326	1.0641	4.252579	7.064175	1.6612
G04	<i>Stat1</i>	6.18543	0.381376	0.0617	0.292716	0.322977	1.1034
G05	<i>Tac1</i>	0.004129	0.003421	0.8285	0.004971	0.006836	1.3753
G06	<i>Tac2</i>	0.109453	0.1233	1.1265	0.032449	0.087683	2.7022
G07	<i>Tek</i>	0.063866	0.071906	1.1259	0.01965	0.027797	1.4146
G08	<i>Tgfb1</i>	0.459285	0.434243	0.9455	0.528079	0.244147	0.4623
G09	<i>Tnf</i>	0.003953	0.008727	2.2076	0.008489	0.003505	0.4129
G10	<i>Trem1</i>	0.001355	0.00346	2.5539	0.00186	0.004084	2.1957
G11	<i>Vcan</i>	0.035597	0.04531	1.2729	0.195373	0.222631	1.1395
G12	<i>Vegfa</i>	0.410015	0.239469	0.5841	0.381138	0.199695	0.5239
H01	<i>Actb</i>	9.019466	10.2603	1.1376	4.170721	7.9003	1.8942
H02	<i>B2m</i>	13.036782	14.385735	1.1035	14.22438	15.725348	1.1055

H03	<i>Gapdh</i>	3.770871	3.655688	0.9695	3.021489	2.509199	0.8305
H04	<i>Gusb</i>	0.121428	0.139193	1.1463	0.134226	0.122357	0.9116
H05	<i>Hsp90ab1</i>	2.257239	2.325719	1.0303	2.088329	1.906602	0.913
H06	<i>MGDC</i>	0.000249	0.000013	0.0535	0.000011	0.000012	1.0754
H07	<i>RTC</i>	1.345201	1.427832	1.0614	1.054064	1.26705	1.2021
H08	<i>RTC</i>	1.489164	1.114812	0.7486	1.56402	1.220352	0.7803
H09	<i>RTC</i>	1.420595	1.39596	0.9827	1.366713	1.288686	0.9429
H10	<i>PPC</i>	3.003496	5.103178	1.6991	4.19393	4.584626	1.0932
H11	<i>PPC</i>	4.629595	4.691311	1.0133	4.304152	4.74989	1.1036
H12	<i>PPC</i>	3.598693	3.503357	0.9735	1.849353	1.506157	0.8144

Supplemental Table S5

Fold-change in Preeclampsia Array gene expression: pooled (n=3) kidney tissue

		E13 PBS	E13 Galectin-7		E17 PBS	E17 Galectin-7	
Well	Gene	2 [^] (-Avg.(Delta(Ct)))		Fold Change	2 [^] (-Avg.(Delta(Ct)))		Fold Change
A01	<i>Abcc1</i>	0.000069	0.000069	0.9996	0.000076	0.000069	0.9054
A02	<i>Abcg2</i>	0.000069	0.000069	0.9996	0.000076	0.000069	0.9054
A03	<i>Adm</i>	0.045624	0.042827	0.9387	0.044808	0.042053	0.9385
A04	<i>Agtr1a</i>	1.607406	1.93213	1.202	0.639664	1.536212	2.4016
A05	<i>Angpt2</i>	0.6569	0.482383	0.7343	0.465059	0.328391	0.7061
A06	<i>Apln</i>	0.633404	0.87887	1.3875	0.948094	0.68221	0.7196
A07	<i>Atp1b1</i>	80.080594	80.403417	1.004	66.732137	60.828709	0.9115
A08	<i>Atp2a2</i>	5.818385	7.531096	1.2944	6.763147	9.598244	1.4192
A09	<i>Bcl6</i>	0.155245	0.110539	0.712	0.108882	0.12116	1.1128
A10	<i>Bhlhe40</i>	0.672325	0.809203	1.2036	1.421871	0.447419	0.3147
A11	<i>C3</i>	0.925179	0.755954	0.8171	0.279906	0.201288	0.7191
A12	<i>Cav1</i>	0.423356	0.874156	2.0648	0.467741	0.35382	0.7564
B01	<i>Ccl12</i>	0.08404	0.051646	0.6145	0.02773	0.022409	0.8081
B02	<i>Cd40lg</i>	0.005505	0.003983	0.7235	0.002573	0.003265	1.2691
B03	<i>Cdh13</i>	0.115863	0.20646	1.7819	0.109041	0.100622	0.9228
B04	<i>Cfd</i>	10.025385	9.114578	0.9091	0.825018	0.686476	0.8321

B05	<i>Clu</i>	15.28248	15.497955	1.0141	15.019395	15.934717	1.0609
B06	<i>Col14a1</i>	1.489369	2.704322	1.8158	0.555483	0.961926	1.7317
B07	<i>Cp</i>	3.071265	2.52564	0.8223	3.545708	2.268728	0.6399
B08	<i>Crh</i>	0.000069	0.000069	0.9996	0.000076	0.000069	0.9054
B09	<i>Crhbp</i>	0.000278	0.001616	5.8159	0.000803	0.000069	0.0861
B10	<i>Cxcl10</i>	0.120857	0.278897	2.3077	0.131314	0.076647	0.5837
B11	<i>Cxcl9</i>	0.011119	0.005972	0.5371	0.000076	0.003446	45.1399
B12	<i>Cxcr4</i>	0.048018	0.108508	2.2597	0.059953	0.096223	1.605
C01	<i>Cyp26a1</i>	0.006655	0.000415	0.0624	0.002692	0.001643	0.6103
C02	<i>Dcn</i>	4.031497	3.381663	0.8388	1.93372	2.216969	1.1465
C03	<i>Dusp1</i>	0.810135	1.462938	1.8058	1.670082	1.232374	0.7379
C04	<i>Edn1</i>	0.042471	0.045091	1.0617	0.016738	0.018422	1.1006
C05	<i>Eng</i>	1.338068	4.121304	3.08	1.175578	1.006782	0.8564
C06	<i>F5</i>	1.665622	0.363851	0.2184	0.245203	0.234455	0.9562
C07	<i>Fabp4</i>	10.495302	7.728685	0.7364	3.487603	2.358856	0.6764
C08	<i>Flt1</i>	0.218944	0.231739	1.0584	0.21916	0.180088	0.8217
C09	<i>Flt4</i>	0.174359	0.213133	1.2224	0.13386	0.150905	1.1273
C10	<i>Fstl3</i>	0.040213	0.011498	0.2859	0.04923	0.062008	1.2595
C11	<i>H2-M3</i>	0.11876	0.11507	0.9689	0.076976	0.085816	1.1148
C12	<i>Hbegf</i>	0.175471	0.066223	0.3774	0.129249	0.09517	0.7363
D01	<i>Hgf</i>	0.182284	0.104653	0.5741	0.063176	0.074753	1.1832

D02	<i>Hif1a</i>	0.971761	1.127704	1.1605	1.072314	1.120289	1.0447
D03	<i>Hp</i>	0.074312	0.102332	1.3771	0.017608	0.022655	1.2866
D04	<i>Hsd17b1</i>	0.001462	0.012609	8.6269	0.005852	0.005507	0.941
D05	<i>Hsp90aa1</i>	5.523022	4.71371	0.8535	4.013102	2.867955	0.7146
D06	<i>Htr3a</i>	0.009018	0.043926	4.871	0.023797	0.023186	0.9743
D07	<i>Htra1</i>	1.109126	0.592181	0.5339	0.908496	2.184976	2.405
D08	<i>lfng</i>	0.001318	0.003704	2.8099	0.002745	0.000964	0.3511
D09	<i>Igf1</i>	0.407211	0.393494	0.9663	0.225989	0.197975	0.876
D10	<i>Igfbp3</i>	11.182685	5.786949	0.5175	11.980463	15.629985	1.3046
D11	<i>Il10</i>	0.000451	0.00089	1.9724	0.000443	0.000069	0.1561
D12	<i>Il11</i>	0.001138	0.001309	1.1503	0.000856	0.001497	1.7476
E01	<i>Il15</i>	0.312345	0.374764	1.1998	0.35429	0.399791	1.1284
E02	<i>Il18</i>	0.040121	0.046741	1.165	0.042328	0.044256	1.0456
E03	<i>Il1a</i>	0.010749	0.060731	5.65	0.011663	0.019105	1.6382
E04	<i>Il2</i>	0.000069	0.000069	0.9996	0.000076	0.000069	0.9054
E05	<i>Il6</i>	0.017921	0.009299	0.5189	0.000076	0.047508	622.3471
E06	<i>Inha</i>	0.014806	0.026051	1.7595	0.00972	0.014373	1.4787
E07	<i>Inhba</i>	0.010016	0.003857	0.3851	0.000076	0.002168	28.4064
E08	<i>Itgb3</i>	0.023018	0.030619	1.3302	0.061945	0.053596	0.8652
E09	<i>Kit</i>	0.185892	0.290555	1.563	0.18558	0.120386	0.6487
E10	<i>Krt19</i>	1.040588	0.249715	0.24	0.77988	0.022514	0.0289

E11	<i>Lep</i>	0.003196	0.001489	0.466	0.000076	0.000339	4.4407
E12	<i>Lpl</i>	7.089814	6.416377	0.905	5.313719	5.509913	1.0369
F01	<i>Mas1</i>	0.014051	0.013551	0.9644	0.011685	0.006359	0.5442
F02	<i>Mmp12</i>	0.029676	0.019557	0.659	0.039745	0.043304	1.0895
F03	<i>Mmp9</i>	0.009123	0.006085	0.667	0.020689	0.009852	0.4762
F04	<i>Ncam1</i>	0.043296	0.030682	0.7087	0.026987	0.078507	2.9091
F05	<i>Ndrp1</i>	38.422508	25.828571	0.6722	28.124583	29.447056	1.047
F06	<i>Nos3</i>	0.043859	0.04509	1.0281	0.026219	0.0255	0.9726
F07	<i>Ntrk2</i>	0.041294	0.03003	0.7272	0.008003	0.003013	0.3765
F08	<i>Pappa2</i>	0.02663	0.012402	0.4657	0.011626	0.016701	1.4365
F09	<i>Pdgfd</i>	0.431731	0.314735	0.729	0.289401	0.274069	0.947
F10	<i>Pgf</i>	0.020114	0.01453	0.7224	0.008646	0.010249	1.1854
F11	<i>Pgr</i>	0.043079	0.072778	1.6894	0.028479	0.04325	1.5187
F12	<i>Qpct</i>	0.159043	0.095488	0.6004	0.077837	0.077454	0.9951
G01	<i>Serpina3n</i>	0.021695	0.040234	1.8545	0.01248	0.009668	0.7747
G02	<i>Sod1</i>	16.265697	17.569886	1.0802	13.807544	18.196366	1.3179
G03	<i>Spp1</i>	76.761754	61.635555	0.8029	60.429613	61.4743	1.0173
G04	<i>Stat1</i>	0.882229	0.696273	0.7892	0.547124	0.424894	0.7766
G05	<i>Tac1</i>	0.072958	0.127475	1.7472	0.000076	0.011147	146.0191
G06	<i>Tac2</i>	0.000206	0.000069	0.3376	0.000134	0.000069	0.5142
G07	<i>Tek</i>	0.429556	0.231127	0.5381	0.269003	0.243789	0.9063

G08	<i>Tgfb1</i>	0.620668	0.508394	0.8191	0.448478	0.392631	0.8755
G09	<i>Tnf</i>	0.013972	0.018509	1.3248	0.022736	0.007452	0.3277
G10	<i>Trem1</i>	0.000069	0.000412	5.9244	0.000076	0.000069	0.9054
G11	<i>Vcan</i>	0.018436	0.010226	0.5547	0.028678	0.015286	0.533
G12	<i>Vegfa</i>	3.660975	2.790253	0.7622	2.954291	2.604652	0.8817
H01	<i>Actb</i>	25.571409	33.548373	1.3119	11.960135	24.391718	2.0394
H02	<i>B2m</i>	23.612924	28.093626	1.1898	20.457314	22.00979	1.0759
H03	<i>Gapdh</i>	39.071934	33.015576	0.845	32.966088	38.406178	1.165
H04	<i>Gusb</i>	0.308923	0.344272	1.1144	0.24665	0.364186	1.4765
H05	<i>Hsp90ab1</i>	12.000851	9.814032	0.8178	11.046304	10.084331	0.9129
H06	<i>MGDC</i>	0.000091	0.000069	0.762	0.000076	0.000069	0.9054
H07	<i>RTC</i>	7.479204	6.87178	0.9188	6.543157	5.695879	0.8705
H08	<i>RTC</i>	6.257064	6.330669	1.0118	12.704712	6.36846	0.5013
H09	<i>RTC</i>	5.960671	4.620999	0.7752	7.838887	6.561608	0.8371
H10	<i>PPC</i>	26.585962	23.966526	0.9015	31.697448	21.539151	0.6795
H11	<i>PPC</i>	23.797032	26.031507	1.0939	28.286108	23.669191	0.8368
H12	<i>PPC</i>	28.356406	17.777233	0.6269	29.672237	22.645987	0.7632

Supplemental Table S6**Primer sequences for human primers.**

Primer	Forward 5'-3'	Reverse 5'-3'
<i>18s</i>	GATCCATTGGAGGGCAAGTCT	CCAAGATCCAACACTACGAGCTT
<i>AGT</i>	CGCCTGCCTGCTGCTGAT	GGAAAGTGAGACCCTCCACCTTGT
<i>ADAM12</i>	GACCTCCCAGAGTTCTGCAC	GCCACAGTTGCCATAAGGAT
<i>FLT-1</i>	CGTAGAGATGTACAGTGAAA	GGTGTGCTTATTTGGACATC
<i>IL11</i>	GTGGCCAGATACAGCTGTCCG	GGTAGGACAGTAGGTCCGCTC
<i>LGALS7</i>	CTTGGTCTGGGTGGTTTCTGA	CCCCGCACAGCAGGTTTA
<i>MMP9</i>	GTATTTGTTCAAGGATGGGAAGTAC	GCAGGATGTCATAGGTCACGTAG
<i>PAPPA2</i>	AGGGGATAGTCCTATTGGGCA	CCTCACCTAGAGACTCCTTGG
<i>SFLT-1-E15A</i>	CTCCTGCGAAACCTCAGTG	GACGATGGTGACGTTGATGT

Supplemental Table S7**Primer sequences for mouse primers.**

Primer	Forward 5'-3'	Reverse 5'-3'
<i>18s</i>	GATCCATTGGAGGGCAAGTCT	CCAAGATCCAACACTACGAGCTT
<i>Ace</i>	AGATATAATGGCTCTCTCAGTG	TTGATGTCATACTCGTAGCC
<i>Ace2</i>	CATTTGCTTGGTGATATGTG	GCCTCTTGAAATATCCTTTCTG
<i>Adam12</i>	TGTGGAAATGGCTATGTGGA	CAGGTGGTAGCGTTACAGCA
<i>Agt</i>	TCCTGACTTGGATAGAGAAC	CTATTGAGAACCTCTCCAC
<i>Agtr1a</i>	AGTTGGGAGGGACTGGATGA	GTTAAGTCCGGGAGAGCAGC
<i>Atp6ap2</i>	AAACAAGAGAACACCCAAAG	TCATATCCAGGATCCATATTCC
<i>Il18</i>	GCTTCAGGCAGGCAGTATC	AGGATGGGCTCTTCTTCAAAG
<i>Il6</i>	TAGTCCTTCTACCCCAATTTCC	TTGGTCCTTAGCCACTCCTTC
<i>Il10</i>	TGGCATGAGGATCAGCAGGG	GGCAGTCCGCAGCTCTAGG
<i>Mme</i>	GAAATTGCCAATGCTACAAC	CTGAATGACTTCCCATTGAC
<i>Mmp9</i>	ATCCAGTATCTGTATGGTCG	TATAGTGGGACACATAGTGG
<i>Renin</i>	GCACCGCTACCTTTGAACGA	CGCCGTAGTACTGGGTATTCA
<i>Vegfr1/Flt-1</i>	GTGATCAGCTCCAGGTTTGACTT	GAGGAGGATGAGGGTGTCTATAGGT
<i>Ywhaz</i>	ACTTAACATTGTGGACATCG	GGATGACAAATGGTCTACTG

Supplemental Table S8**Proteins in cultured placental villi explant conditioned media (hypoxia: 2% O₂) significantly regulated by galectin-7 treatment.**

Gene ID	Protein	Mol Weight (kDa)	Unique peptides	Sequence coverage %	LFQ Intensity Mean+sem	Fold change from control
PLG	Plasminogen	90.568	25	33.8	C: 23.5 [^] G: 21.3+0.1	0.219
SERPINC1	Antithrombin-III	52.602	9	30.2	C: 22.1+0.6 G: 19.8+0.1	0.209
AGT	Angiotensinogen	53.154	8	23.1	C: 21.9+0.5 G: 20.6+0.2	0.393
CGA	Glycoprotein hormones alpha chain	13.075	3	23.3	C: 24.5+0.2 G: 26.5 [^]	3.921
COL3A1	Collagen alpha-1(III) chain	138.56	33	30.2	C: 24.5+0.1 G: 25.4+0.3	1.870
VTN	Vitronectin	54.305	7	19	C: 22.6 [^] G: 20.7+0.2	0.270
LDHB	L-lactate dehydrogenase B chain	36.638	11	34.4	C: 25.3+0.1 G: 25.9+0.1	1.473
LAMB1	Laminin subunit beta-1	198.04	21	11.1	C: 19.0 [^] G: 20.4+0.3	2.5782

[^], detected in only 2/3 samples by proteomics.

Supplemental Figure S1

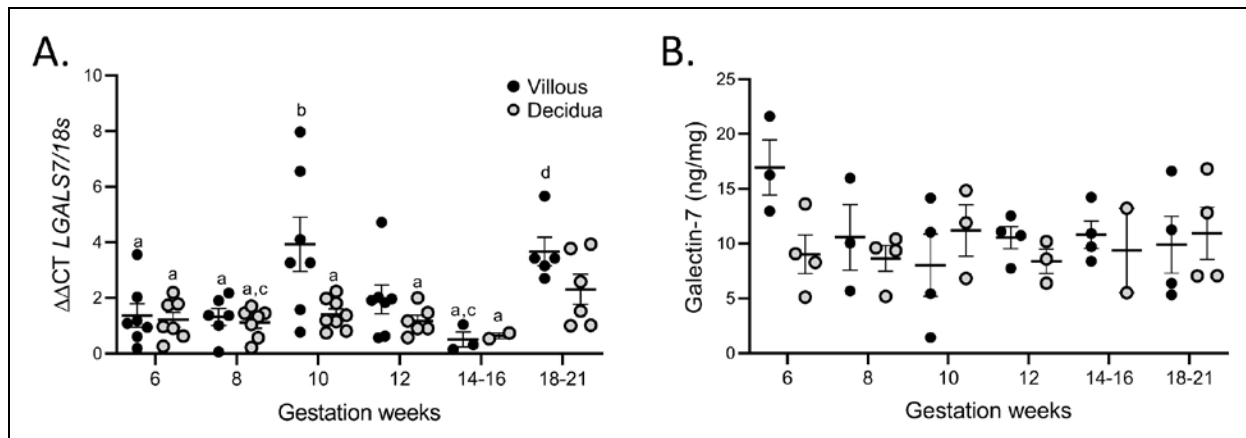


Figure S1. A. *LGALS7* expression in human first- and second-trimester placental villous and decidua. a is significantly different to b, c is significantly different to d, $P < 0.05$, Two-way ANOVA with Sidak's multiple comparisons test, $n = 2-8$ /group. B. Galectin-7 concentration in first- and second-trimester placental villous and decidua. $n = 2-4$ /group. Data are presented as mean \pm SEM.

Supplemental Figure S2

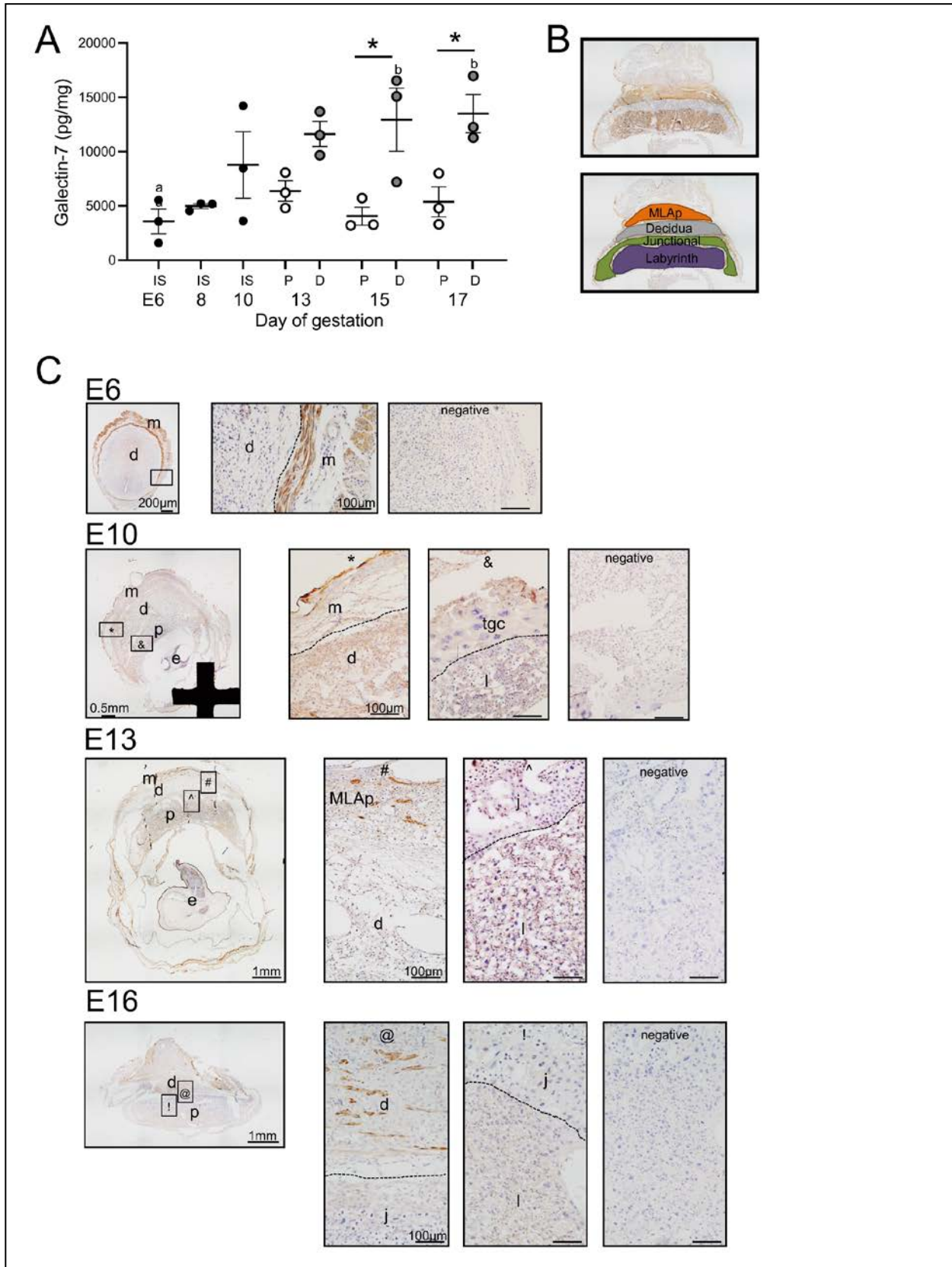


Figure S2. Galectin-7 expression in wild-type mouse implantation sites. A. Galectin-7 protein in wild-type mouse implantation sites, placenta and decidua across gestation quantified by ELISA. Images show ISB4 staining of the placenta to identify representative zones of the placenta (labyrinth [purple], junctional [green]), decidua (grey) and metrial lymphoid aggregate of pregnancy (MLAp [orange]) as defined in this study. a is significantly different to b, $*P < 0.05$, Two-way ANOVA, $n = 3-4$ /group. D, decidua; E, embryonic day; IS, implantation site; P, placenta. B. Galectin-7 immunolocalization in wild-type implantation sites across gestation. Dashed line indicates separation between zones; d, decidua; e, embryo; j, junctional zone; l, labyrinth; m, myometrium; p, placenta; tgc, trophoblast giant cells. *, &, #, ^, ! and @ indicate matched images between low power (on left) and higher power (on right).

Supplemental Figure S3

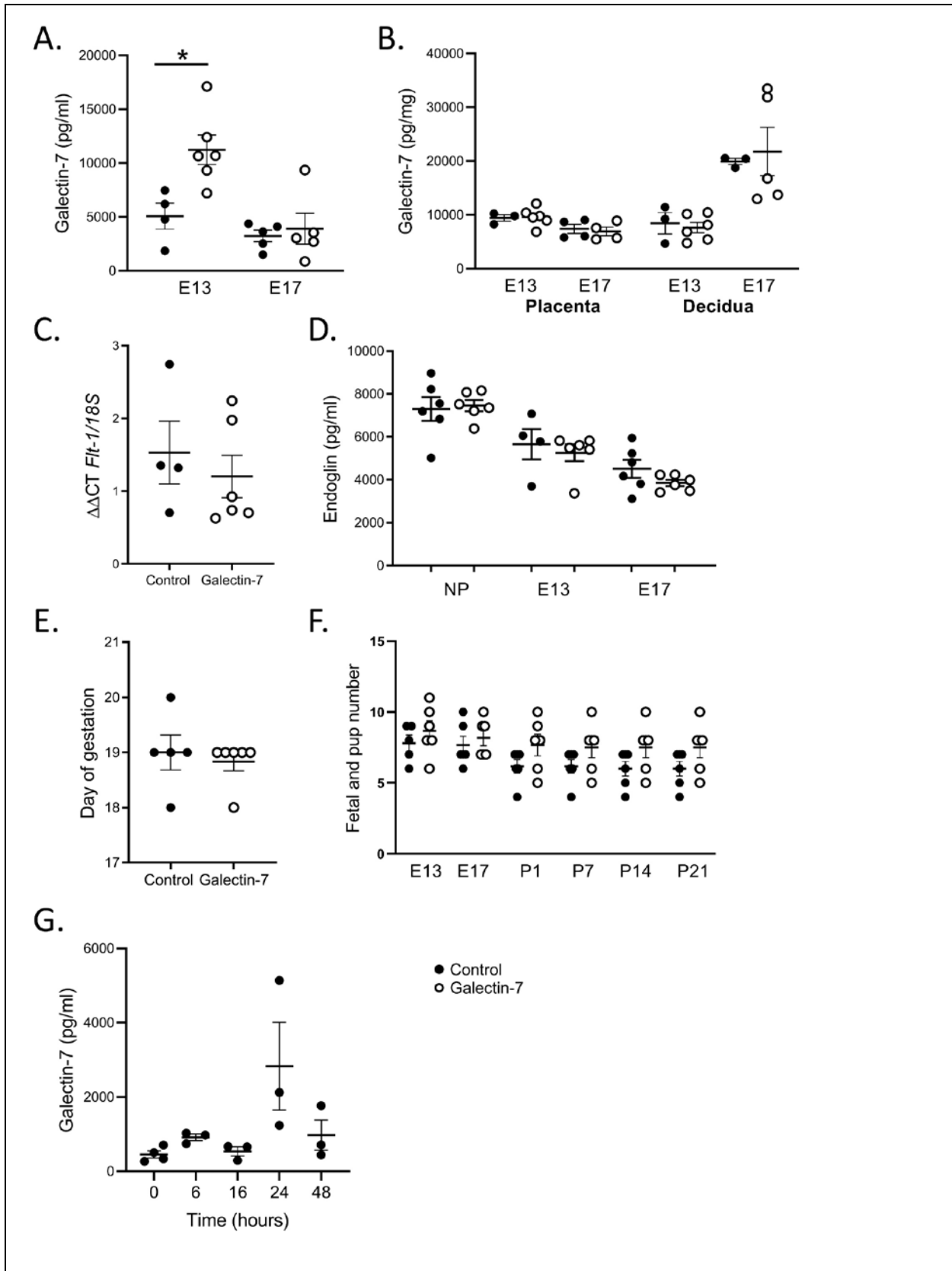


Figure S3. Mouse *in vivo* features following galectin-7 administration (E8-12) to pregnant mice. A. Galectin-7 protein levels in serum at E13 and E17 quantified by ELISA. * $P < 0.05$, Student's t-test, $n = 4-6$ /group. B. Galectin-7 protein levels in placenta and decidua at E13 and 17 were quantified by ELISA. Student's t-test, $n = 3-5$ /group. C. *Flt-1* mRNA expression in mouse placenta at E17. Student's t-test, $n = 4-6$. D. Serum levels of endoglin were quantified by ELISA. One-way ANOVA, $n = 3-6$. E. Day of birth following galectin-7 administration. F. Fetal and pup number across gestation following galectin-7 administration. G. Serum retention of a single dose of recombinant human galectin-7 (400 μ g/kg) administered to non-pregnant female mice. Galectin-7 levels in serum at up to 48h after administration were quantified by ELISA. One-way ANOVA, $n = 3$ /group. Data are presented as mean \pm SEM. E, embryonic day; NP, non-pregnant; P, post-natal day.

Supplemental Figure S4

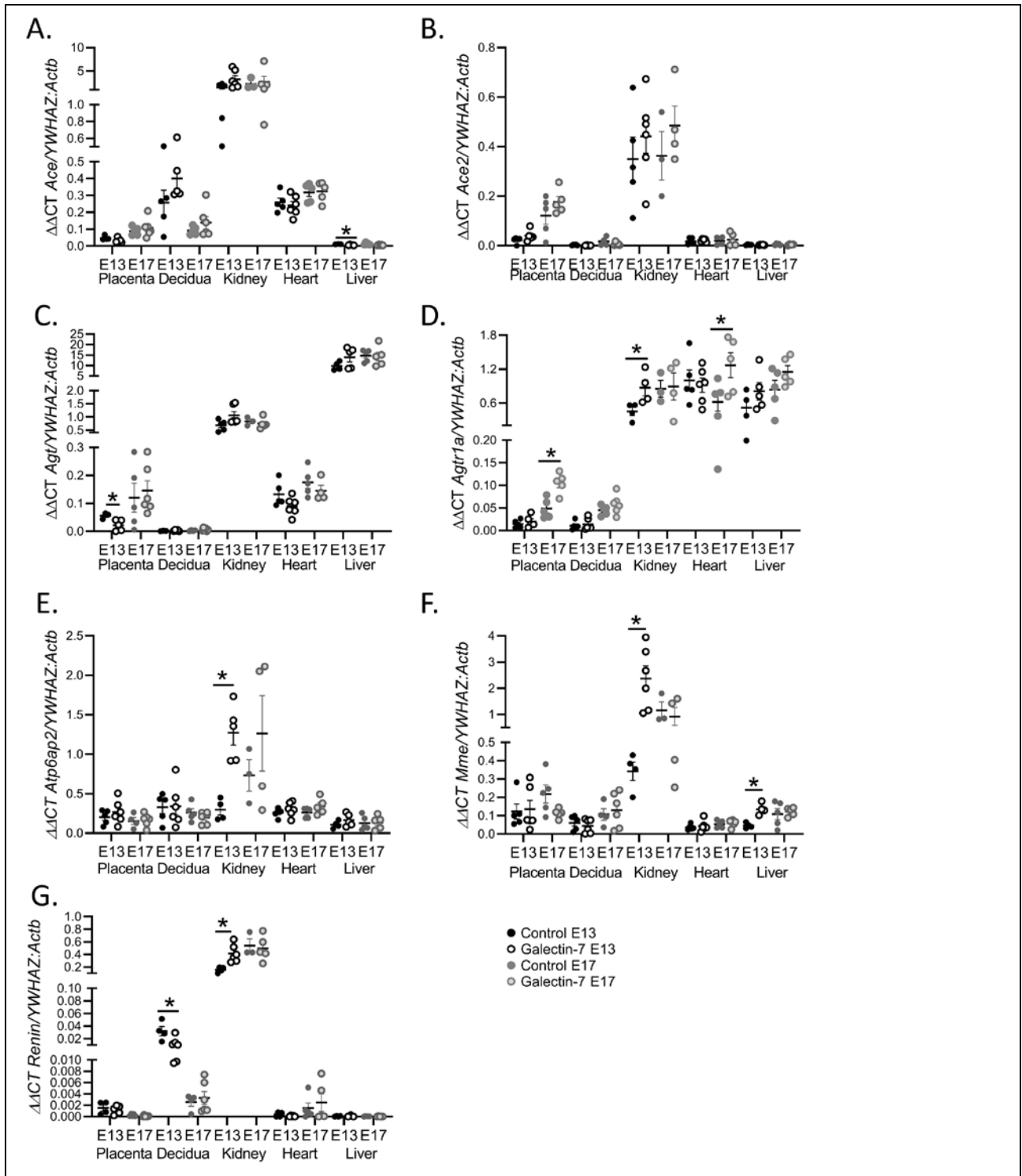


Figure S4. Renin-Angiotensin system factor expression in pregnant mouse tissues following galectin-7 administration (E8-12). A. *Ace* B. *Ace2* C. *Agt* D. *Agtr1a* E. *Atp6ap2* F. *Mme* G. *Renin* expression was quantified by RT-qPCR in placenta, decidua, kidney, heart and liver at E13 and E17. *P<0.05, Student's t-test, n=3-6. Data are presented as mean±SEM. E, embryonic day.

Supplemental Figure S5

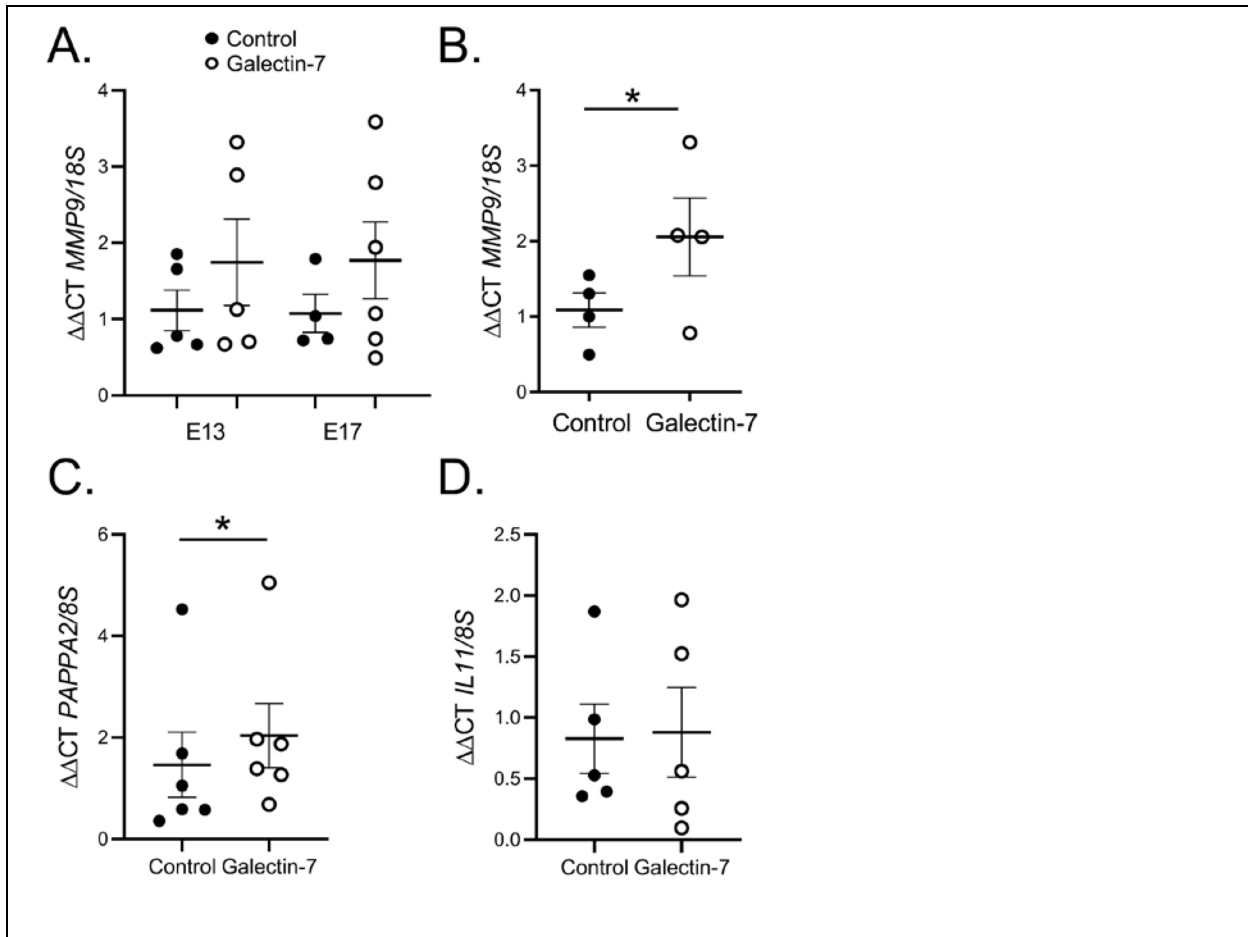


Figure S5. Galectin-7 regulates placental production of key regulators of trophoblast invasion A. *Mmp9* mRNA expression in mouse placenta at E13 and E17. * $P < 0.05$, Student's t-test, $n = 3-6$. B. Human recombinant galectin-7 ($1 \mu\text{g/ml}$) was confirmed as active in mouse cells by quantifying *MMP9* mRNA expression (TCMK1 cells) after 6.5h treatment. * $P < 0.05$, ratio paired t-test, $n = 4$. Effect of recombinant human galectin-7 treatment ($1 \mu\text{g/ml}$) on human trophoblast *in vitro*. C. *IL11* mRNA expression was quantified by RT-qPCR in first-trimester human placental villous explants cultured for 16h under low oxygen conditions ($2\%O_2$) and treated with recombinant human galectin-7 ($1 \mu\text{g/ml}$) or vehicle control. $n = 4$. D. *PAPP2* mRNA expression was quantified by RT-qPCR in first-trimester human placental villous explants cultured for 16h under low oxygen conditions ($2\%O_2$) and treated with recombinant human galectin-7 ($1 \mu\text{g/ml}$) or vehicle control. * $P < 0.05$, paired t-test, $n = 6$. Data are presented as mean \pm SEM. E, embryonic day.



Minerva Access is the Institutional Repository of The University of Melbourne

Author/s:

Menkhorst, E; Zhou, W; Santos, LL; Delforce, S; So, T; Rainczuk, K; Loke, H; Syngelaki, A; Varshney, S; Williamson, N; Pringle, K; Young, MJ; Nicolaidis, KH; St-Pierre, Y; Dimitriadis, E

Title:

Galectin-7 Impairs Placentation and Causes Preeclampsia Features in Mice

Date:

2020-10-01

Citation:

Menkhorst, E., Zhou, W., Santos, L. L., Delforce, S., So, T., Rainczuk, K., Loke, H., Syngelaki, A., Varshney, S., Williamson, N., Pringle, K., Young, M. J., Nicolaidis, K. H., St-Pierre, Y. & Dimitriadis, E. (2020). Galectin-7 Impairs Placentation and Causes Preeclampsia Features in Mice. *Hypertension*, 76 (4), pp.1185-1194.
<https://doi.org/10.1161/HYPERTENSIONAHA.120.15313>.

Persistent Link:

<http://hdl.handle.net/11343/268162>

File Description:

Accepted version